

Spring 2020

## Identifying and Characterizing Transgenic Lines That Drive Gene Expression in the Adult Fat Body of the *Drosophila Melanogaster*

Michael Edward Meyerink

Follow this and additional works at: <https://scholarcommons.sc.edu/etd>



Part of the [Biology Commons](#)

---

### Recommended Citation

Meyerink, M. E.(2020). *Identifying and Characterizing Transgenic Lines That Drive Gene Expression in the Adult Fat Body of the Drosophila Melanogaster*. (Master's thesis). Retrieved from <https://scholarcommons.sc.edu/etd/5711>

This Open Access Thesis is brought to you by Scholar Commons. It has been accepted for inclusion in Theses and Dissertations by an authorized administrator of Scholar Commons. For more information, please contact [dillarda@mailbox.sc.edu](mailto:dillarda@mailbox.sc.edu).

IDENTIFYING AND CHARACTERIZING TRANSGENIC LINES THAT DRIVE GENE  
EXPRESSION IN THE ADULT FAT BODY OF THE *DROSOPHILA MELANOGASTER*

by

Michael Edward Meyerink

Bachelor of Science  
University of South Carolina, 2018

---

Submitted in Partial Fulfillment of the Requirements

For the Degree of Master of Science in

Biological Science

College of Arts and Science

University of South Carolina

2020

Accepted by:

Alissa Armstrong, Major Professor

Carol Boggs, Committee Member

Alan Waldman, Committee Member

Cheryl L. Addy, Vice Provost and Dean of the Graduate School

© Copyright by Michael Edward Meyerink, 2020  
All Rights Reserved.

## DEDICATION

I would like to dedicate this thesis to my family, friends and colleagues. The decision to pursue this project was enlightening and I bumped my head a quite a few times along the way. Without them this work would have been almost impossible to complete. I am forever grateful that they were in my corner every step of the way.

## ACKNOWLEDGEMENTS

I would like to acknowledge all my colleagues in the Armstrong laboratory; Tanica Bradshaw, Chad Simmons, and Dr. Subhshri Sahu. They were incredible mentors and support and aided me tremendously in my experiments. Additionally, I would like to thank my Thesis committee: Dr. Alissa Armstrong, Dr. Carol Boggs, and Dr. Alan Waldman. They all provided excellent feed back to my work and kept me on track when I felt astray.

## ABSTRACT

Adult *Drosophila Melanogaster* is a powerful model organism in genetic studies and has high tissue and gene homology to humans. Like humans, *Drosophila* tissues communicate in order to respond to physiological stimuli, such as diet, aging, and disease. The fat body, homologous to human adipocytes and hepatocytes, functions as both an endocrine and energy storage organ; and has been shown to play a critical role in many metabolic processes. The aim of this study is to characterize differences in fat body gene expression to ultimately identify if there are subpopulations of adipocytes with different functions related to fat body communication to other tissues. To do so, nine fly lines with a genetic insertion of *Gal4*, which encodes a transcription factor, under the influence of a tissue specific promoter, were mated with a fly line that encodes membrane bound green fluorescent protein under the control of UAS, the DNA sequence recognized by *Gal4*. Progeny containing both genetic elements will have cells that fluoresce green, GFP, at the cell membrane in tissues or cells where the promoter is active. This study reports that five of the nine *Gal4* lines tested, with promoter sequences reported to be actively expressed in larval adipocytes, drive UAS-GFP expression in adult adipocytes, with distinct levels of gene expression. Three of the five lines were more carefully examined to uncover a link between level of gene expression and adipocyte size. These three lines, *c754-Gal4*, *ppl-Gal4*, and *Lsp2(3.1)-Gal4*, drove robust GFP expression in adult adipocytes. *Lsp2(3.1)-Gal4* showed the strongest GFP expression, while expression levels for *c754-Gal4* and *ppl-Gal4* were comparable to each other. When correlating GFP

intensity with adipocyte perimeter, a correlation was found with gene expression and adipocyte size for two of the three lines. In order to identify the causality between cell size on gene expression the data was further analyzed using a linear regression model. This information indicated that specific promoters and their corresponding genes are differentially expressed based on cell size. Altogether, I have identified at least one transgenic line, *c754-Gal4*, that was not previously known to promote gene expression in adult adipocytes and ruled out transgenic lines, *Lsp2-Gal4.H*, *c591-Gal4*, *l(2)T76<sup>T76</sup>-Gal4*, *c855a-Gal4*, *C833-Gal4* that do not drive gene expression in the fat body of adult female flies. In the future, a full-body analysis in addition to an examination of other organelle characteristics will lead to a more comprehensive understanding of adipocyte functionality with respect to inter-tissue communication.

## TABLE OF CONTENTS

Dedication.....	iii
Acknowledgements .....	iv
Abstract.....	v
List of Figures.....	ix
Chapter 1: Introduction.....	1
1.1 Adult Stem Cells Maintain Tissue Homeostasis .....	1
1.2 Interorgan Communication and The Characterization of The Adult <i>Drosophila</i> Fat Body.....	3
Chapter 2: Materials and Methods .....	6
2.1 The GAL4/UAS System to Assess Gene Expression in The Adult Fat Body ..	6
2.2 Whole Mount Immunostaining of Adult <i>Drosophila</i> Adipose Tissue.....	9
2.3 Measurements of Gene Expression Level and Adipocyte Size.....	10
2.4 Data Analysis.....	10
Chapter 3: Results .....	12
3.1 <i>Lsp2(3.1)-Gal4</i> Drives Robust Gene Expression in Adult Fat.....	12
3.2 <i>Ppl-Gal4</i> Drives Moderate Gene Expression in Adult Fat .....	14
3.3 <i>C564-Gal4</i> Drives Moderate Gene Expression in Adult Fat .....	16
3.4 <i>C754-Gal4</i> Drives Low Gene Expression in Adult Fat .....	18
3.5 Five <i>Gal4</i> Lines Did Not Drive Expression in The Adult Fat Body .....	20
Chapter 4: Gene Expression and Cell Morphology .....	27



4.1 Comparison of Gene Expression of Adult Fat body Drivers .....	27
4.2 Gene Expression with Respect to Cell Size .....	31
4.3 Comparing Regressions Among Transgenic Driver Lines.....	37
Chapter 5: Discussion.....	40
References.....	44

## LIST OF FIGURES

Figure 2.1 <i>UAS/GAL4</i> system schema .....	7
Figure 3.1 <i>tubP-Gal80ts; 3.1Lsp2-Gal4/TM6b &gt; w*; P{10XUAS-mCD8::GFP}attP2</i> ...	13
Figure 3.2 <i>w*; P{ppl-GAL4.P}2 &gt; w*; P{10XUAS-mCD8::GFP}attP2</i> .....	15
Figure 3.3 <i>w<sup>1118</sup>; P{GawB}c564 &gt; w*; P{10XUAS-mCD8::GFP}attP2</i> .....	17
Figure 3.4 <i>P{GawB}c754, w<sup>1118</sup> &gt; w*; P{10XUAS-mCD8::GFP}attP2</i> .....	19
Figure 3.5 <i>y1 w<sup>1118</sup>; P{Lsp2-GAL4.H}3 &gt; w*; P{10XUAS-mCD8::GFP}attP2</i> .....	21
Figure 3.6 <i>w<sup>1118</sup>; P{GawB}C833 &gt; w*; P{10XUAS-mCD8::GFP}attP2</i> .....	23
Figure 3.7 <i>w<sup>1118</sup>; P{GawB}C855a &gt; w*; P{10XUAS-mCD8::GFP}attP2</i> .....	24
Figure 3.8 <i>w*; P{GawB}c591 &gt; w*; P{10XUAS-mCD8::GFP}attP2</i> .....	25
Figure 3.9 <i>w<sup>1118</sup>; P{GawB}l(2)T76T76/CyO &gt; w*; P{10XUAS-mCD8::GFP}attP2</i> .....	26
Figure 4.1 Average GFP intensity of each individual cross .....	29
Figure 4.2 Tukey's range test between genotypes 1 .....	30
Figure 4.3 <i>w<sup>1118</sup> &gt; UAS-mCD8::GFP</i> GFP intensity vs perimeter.....	33
Figure 4.4 <i>Lsp2(3.1)-GAL4 &gt;x UAS-mCD8::GFP</i> GFP intensity vs perimeter.....	34
Figure 4.5 <i>Ppl-GAL4 &gt; UAS-mCD8::GFP</i> GFP intensity vs perimeter.....	35
Figure 4.6 <i>c754-GAL4 &gt; UAS-mCD8::GFP</i> GFP intensity vs perimeter.....	36
Figure 4.7 Compiled regressions of each individual cross .....	38
Figure 4.8 Tukey's range test between genotypes 2 .....	39

## LIST OF ABBREVIATIONS

BSA	Bovine serum albumin
DAPI	4',6-diamidino-2-phenylindole
ISC	Intestinal Stem Cells
LIF	Leukemia inhibitory factor
Lsp2	Larval Serum Protein 2
NGS	Normal Goat Serum
PBS	Phosphate Buffer Saline
PBT	Phosphate Buffer Tween-20
Ppl	Pumpless
TGF- $\beta$	Transforming growth factor beta
TOR	Target of Rapamycin
UAS	Upstream Activating Sequence
Wnt	Wingless-related integration site

## CHAPTER 1

### INTRODUCTION

#### 1.1 ADULT STEM CELLS MAINTAIN TISSUE HOMEOSTASIS

The human body has an exceedingly high durability and adaptability. The effects of stress, diet, and illness are constantly degrading normal physiology; all the while, our organs are consistently addressing these effects to keep the body functional and healthy. In order to do so, the body has developed multiple methods of sustentation. One specific mechanism of which, is the maintenance of high turnover organ systems with adult stem cells.

For example, in humans, the small intestine houses a stem cell niche in what is known as the intestinal crypt (Umar 2010). These intestinal stem cells (ISCs) can proliferate and differentiate into enterocytes and goblet cells, both of which are specialized cells that aid in the secretory and absorptive function of the small intestine (Santos et. al 2018). These cells are constantly being replenished and without ISC's enterocytes and goblet cells, as well as the structural integrity of the organ, would begin to malfunction. Additionally, in the bone marrow, there resides two specific adult stem cell lineages, hematopoietic stem cells and mesenchymal stem cells (Laquinta et al 2019). Hematopoietic stem cells support development of erythrocytes and leukocytes which supply oxygen as well as immunity to our tissues respectively (Bresnick et al. 2018; Mahla 2016). Mesenchymal stem cells support development into osteoblasts which later go one to form the bone matrix of the skeletal system (Laquinta et al 2019).

Stem cell populations make use of a variety of well characterized signaling pathways to maintain tissue homeostasis. Signaling pathways such as TGF- $\beta$ . (Transforming growth factor beta), Wnt (Wingless-related integration site) and LIF (Leukemia inhibitory factor), affect the activity of stem cells by modulating their quiescence and pluripotency (Bhavanasi and Klein 2016; Bieberich and Wang 2013). Moreover, adult stem cells are affected by broader organismal physiology such as responding to disease, physical activity and most importantly nutrition. Stem cells are heavily modulated by diet, as these cells need energy in order to maintain functionality and structural integrity (Mihaylova et al. 2014). Given the current obesity epidemic, with approximately 40% of US adults being obese (Hales et al., 2017), understanding the cellular and molecular responses of adult stem cells to nutritional status is an area of research importance. The Armstrong Laboratory is particularly interested in how adipose tissue communicates with tissues supported by adult stem cell populations.

Diet affects the functionality of every tissue, even those not supported by stem cells (Ohlhorst et al 2013). If key nutrients are not available or if there is an overabundance of a single macromolecule, the body will begin to breakdown in functionality and key metabolic processes will begin to stall. For example, in humans, excessive consumption in high fat or processed foods leads to obesity and other co-morbidities, such as heart disease and diabetes (Haslam and James 2005). While a diet that is well balanced, in addition to exercise, keeps the body functional and promotes a longer life span (Ford et al. 2011). In fact, nutrition has an immense impact on how tissues interact and communicate with one another, modulating their function depending on nutrient availability (Castillo-Armengol et al. 2019). However, the exact molecular

means on how this communication is perturbed in cases of obesity or malnutrition is not known, and therefore understanding it will provide a more robust comprehension on nutrition's effects on organismal homeostasis as whole.

## 1.2 INTERORGAN COMMUNICATION

### AND THE CHARACTERIZATION OF THE ADULT *DROSOPHILA* FAT BODY

In order to study interorgan cross talk I have utilized *Drosophila Melanogaster*, a model organism that is known to reproduce quickly and in high volume. This organism can develop from an egg to adult in approximately 10 days at 25°C (Hales et al 2015). In addition, *Drosophila* has an incredibly high fecundity, yielding many progeny in short amount of time over several of generations (Hales et al 2015). Furthermore, *Drosophila Melanogaster* shares many organ systems with humans, containing cardiovascular, excretory, digestive, and most importantly adipose tissues (Gáliková and Klepsatel 2018). Over 75% of genes that cause disease in humans have homologs that are found in the fruit fly, and key metabolic pathways, such as insulin signaling are conserved as well (Brogiolo et al., 2001; Pandey and Nichols 2011). Lastly, many critical studies have utilized the *Drosophila* model to serve as the basis for key findings in higher level organisms, including humans (Greene et al.2003; Koh et al. 2006; Pesah et al. 2004).

Given the potential for communication to and from several tissues, isolating the interaction between a pair of tissues will allow us to investigate the phenomenon of interorgan communication. The initial focus of the Armstrong laboratory centers around crosstalk between the ovary and the fat tissue. Previous studies have shown that the *Drosophila* fat body, analogous to mammalian adipose and liver tissue, communicates organismal nutrient status with the ovary in adult females. By modifying amino acid

sensing in *Drosophila* fat tissue, it was found that adipocytes use the amino acid response pathway to regulate germline stem cell maintenance while using TOR-mediated signaling to promote germline cell number and ovulation in the ovary (Armstrong et al. 2014). Additionally, reduction of insulin signaling in adipocytes also affected female reproductive health negatively by leading to reduced germline cell survival, vitellogenesis, and germline stem cell number (Armstrong and Drummond-Barbosa, 2018). While these previous studies show that the fat body employs nutrient sensing pathways to communicate with the ovary, it is unknown if particular subsets of adipocytes mediate the specificity of each pathway on distinct aspects of oocyte development.

The adult *Drosophila* fat body occupies three anatomical positions: the head, thorax and abdomen. The abdomen contains the largest fat body mass with respect to the other two positions and is comprised of two distinct cell types: oenocytes and adipocytes. The former, analogous to mammalian liver tissue, metabolize lipids and performs detoxification (Droujinine and Perrimon 2016; Makki et al. 2014). While the latter acts as both an energy storage and endocrine organ, storing excess nutrients and dispersing them to other tissues, as well as secreting adipokines to communicate nutrient uptake to said tissues (Arrese and Soulages 2010; Droujinine and Perrimon 2016).

It has been shown in previous studies that the fat body in other insects can be characterized differently. In *Helicoverpa zea* prepupae, regional distinctions are defined as the perivisceral fat body and peripheral fat body which differ based on protein and lipid content (Hauerland and Shirk 1995). These regional distinctions can be further differentiated by their ultrastructural characteristics. Cells in the perivisceral fat body

contain enlarged lipid droplets, while the peripheral fat body has enlarged autophagic vacuoles (Haunerland and Shirk, 1995). Thus, the *Drosophila* fat body may be morphologically regionalized in a similar manner.

Moreover, evidence suggests that the adult *Drosophila* fat body is functionally regionalized. When the transcription factor FOXO, whose function is normally suppressed by insulin signaling, is conditionally expressed in the head fat there is an increase in organismal lifespan; however, when expressed in the abdominal fat the effect on lifespan is absent (Hwangbo et al., 2004). While there is some indication of the morphological and functional regionalization of the adult fat tissue in *Drosophila*, the cellular and molecular underpinnings of these differences remain largely unexplored. The purpose of the work described in this study is to identify and characterize sub-populations of adipocytes in the fly adipose tissue.

In order to address this issue, I have utilized a transgenic approach that allows characterization of several fly lines that are known to promote gene expression in the larval fat body. As a first step, I set out to identify which of these transgenic lines also promote gene expression in the adult fat body. Second, gene expression levels were compared across transgenic lines to get an idea of differences in molecular signatures of adipocytes. Lastly, a subset of these lines were more carefully analyzed to identify any relationship between gene expression level and cell size. These methods allow for the study of the separate segments of tissue and can elucidate if those different segments have varying levels of genetic expression. This can ultimately identify if there are subpopulations of adipocytes that may have different functions related to fat body communication to other tissues.



## CHAPTER 2

### MATERIALS AND METHODS

#### 2.1 THE *GAL4/UAS* SYSTEM TO ASSESS GENE EXPRESSION IN THE ADULT FAT BODY

In order to identify lines that promote gene expression in the adult fat body, the UAS-Gal4 system was used (Osterwalder et al. 2001). This molecular system offers a way to selectively stimulate gene expression in a cell type- and/or tissue-specific manner utilizing two genetic constructs derived from yeast. The first line, known as a driver, has a transgenic insertion with the *Gal4* gene sequence under the control of a native, tissue specific, promoter/enhancer sequence. The second fly line has an upstream activating sequence (*UAS*), which is recognized by the transcription factor Gal4, upstream of a specific gene of interest. For my work, the gene of interest is *mCD8::GFP*; a gene which encodes a cell membrane surface protein with a green fluorescent protein tag. The *UAS-mCD8::GFP* sequence can only be expressed when recognized by Gal4 protein encoded by the *Gal4* gene. In flies containing both transgenes, as a result of standard genetic crosses, Gal4 protein binds to the *UAS* sequence, thus promoting tissue specific expression of GFP at the cell membrane (See Figure 2.1).

The following transgenic fly lines were used: 1)  $w^{1118}; tubP-Gal80^s; Lsp2(3.1)-Gal4/TM6B$ , 2)  $ppl-Gal4$ , 3)  $P\{GawB\}c754;w^{1118}$ , 4)  $w^{1118}; P\{GawB\}c564$ , 5)  $w^{1118}; P\{GawB\}l(2)T76T76/CyO$ , 6)  $w^{1118}; P\{GawB\}C833$ , 7)  $w^{1118}; P\{GawB\}C855a$ , 8)  $w^*$ ;  $P\{GawB\}c591$ , 9)  $y^l w^{1118}; P\{Lsp2-GAL4.H\}3$ , and 10)  $w^*$ ;  $P\{10XUAS-$

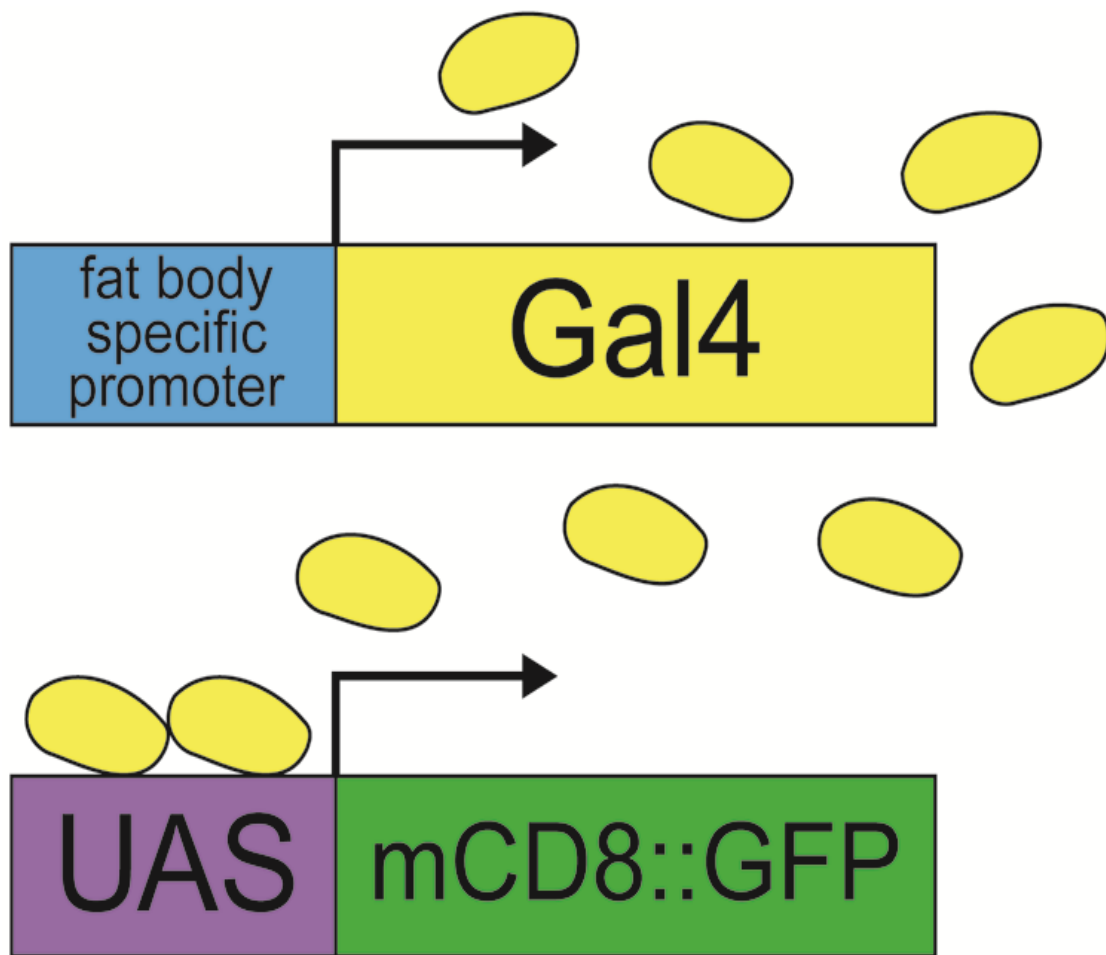


Figure 2.1 *UAS/GAL4* system schema: A tissue specific promoter is conjoined with a *GAL4* coding region. The Upstream activating sequence, which is upstream of a transgene of interest, will only activate if Gal4 is encoded and binds with the upstream activating sequence.

*mCD8::GFP}attP2* (Vienna *Drosophila* Resource Center; Bloomington *Drosophila* Stock Center). All fly lines were reared at 25°C in vials containing Nutri-Fly® BF fly food (Genesee Scientific). The driver lines were transferred to fresh food vials monthly, while control lines, *w<sup>1118</sup>* (negative control), *tubP Gal80ts;Lsp2(3.1)-Gal4/TM6B* (positive control), *ppl-Gal4* (positive control) were transferred to fresh food weekly.

To generate transgenic lines containing the *Gal4* and *UAS* genetic elements, ten male flies from the corresponding driver/control lines and ten female flies from the *UAS-mCD8::GFP* line were added into fresh vials containing Nutri-Fly® BF and additional dry yeast pellets, in duplicate. These crosses were then maintained at 29°C and flipped into freshly yeasted vials every two-three days for four consecutive flips or until the initial driver and reporter flies were exhausted. After approximately eight days, first generation progeny containing the appropriate transgenes (as determined by the presence or absence of phenotypic markers) were collected in a fresh vial and maintained for two-three days at 29°C, to insure degradation of larval fat. They would then be flipped into a fresh vial with wet yeast for one additional day prior to dissection.

## 2.2 WHOLE MOUNT IMMUNOSTAINING OF ADULT *DROSOPHILA* ADIPOSE TISSUE

For each adult fly the head and thorax was removed leaving only the abdomen. The abdominal carcass was dissected, splitting the ventral tissue longitudinally to reveal the fat body located on the dorsal portion of the abdomen, in Grace's media (Caisson Laboratories). These abdominal carcasses were then fixed in 5.3% formaldehyde for 20 minutes at room temperature (25°C). Samples were rinsed and washed in Phosphate buffered saline (PBS) containing 0.5% tween-20 detergent (PBT). Samples were then blocked overnight in 0.5% PBT containing 5% bovine serum albumin (BSA) and 5% normal goat serum (NGS) at 4°C. The abdominal carcasses were then incubated in primary antibodies overnight at 4°C, and secondary antibodies for 2 hr at room temperature after three consecutive washes. Tissues were then mounted in Vectashield® mounting medium containing DAPI. Abdomens were then scraped for adipocytes and placed on microscope slides. Fluorescent images were collected on a Zeiss 800 LSM confocal laser scanning microscope at 20 x magnification. The following primary antibodies were used: mouse anti-alpha spectrin (Developmental Studies Hybridoma Bank; 323 or M10-2), chicken anti-GFP (abcam; ab13970), Alexa Fluor™ Plus 647 Phalloidin (ThermoFischer Scientific). The following secondary antibodies, all from Invitrogen, were used: goat anti-rabbit mAb (Alexa Fluor 647 conjugate), goat anti-mouse Alexa Fluor 647, goat anti-chicken Alexa Fluor 568.

### 2.3 MEASUREMENTS OF GENE EXPRESSION LEVEL AND ADIPOCYTE SIZE

Adipocytes for each genetic cross were measured utilizing Zen Blue 3.0 measurement software. A spline contour was drawn around the adipocyte of interest, acquiring the average fluorescent signal intensity for the endogenous cell membrane GFP and perimeter. The software measures the intensity of GFP by collecting the average pixel intensity of the defined drawn area of the 488 nm channel, thus every individual measurement is the average GFP signal of a defined adipocyte. Cells were measured in reference to anti-alpha spectrin staining around the cell membrane (in micrometers).

### 2.4 DATA ANALYSIS

The average GFP intensity for each transgenic cross was plotted into a bar graph in Graph Pad Prism. To compare the levels of gene expression between the genotypes, an ANOVA was performed utilizing the average GFP intensity of each transgenic cross as the dependent variable and the genotype as the independent variable. To compare each genotype individually, a post hoc Tukey's range test was performed for the average GFP intensities.

To identify if there was causal relationship between the level of gene expression and cellular size, linear regressions were constructed for each genotype with the average GFP intensity plotted as a function of cell size in Graph Pad Prism.

To compare the relationship of cell size on the level of gene expression between genotypes, the regressions were plotted on a single graph. Graph Pad Prism cannot compare multiple linear functions at once, therefore to work around this an ANOVA was performed using the expression level over the cell size (the slope) for each

regression as the dependent variable and the genotype as the independent variable (<https://www.graphpad.com/>). To compare each genotype individually, a post hoc Tukey's range test was performed comparing the slopes for each regression.

## CHAPTER 3

### RESULTS

#### 3.1 *LSP2(3.1)-GAL4* DRIVES ROBUST GENE EXPRESSION IN ADULT FAT

*TubP-Gal80<sup>ts</sup>; 3.1Lsp2-Gal4/TM6b* is a transgenic line with the *Gal4* insertion located on the second chromosome. This insertion is under the control of the 3.1 Kb *Lsp2(3.1)* promoter which has been shown to drive expression exclusively in the adult fat body (Lazareva et al. 2007). The promoter *Lsp2* controls expression of the larval serum protein 2 gene which has been reported to be involved with motor neuron axon guidance, synaptic target inhibition in the larval stages, and as a component of larger larval serum complex (Inaki et al 2007; Brock and Roberts 1980).

*Lsp2(3.1)-Gal4* is a robust driver of gene expression in the adult fat body. When crossed with *UAS-MCD8::GFP*, adipocytes show high levels of GFP expression around the cell membrane which is evenly distributed among patches of adipocytes (Figure 3.1). Though individual cells may vary in size and shape, GFP intensity surrounding the cell membrane appears to be equivalent. There have been slight variations in individual cases, where some patches of adipocytes have little to no expression, however these cases are rare and inconsistent. Overall, *tubP-Gal80<sup>ts</sup>; 3.1Lsp2-Gal4/TM6b* appears to be an exceptional driver of gene expression in the adult fat body.

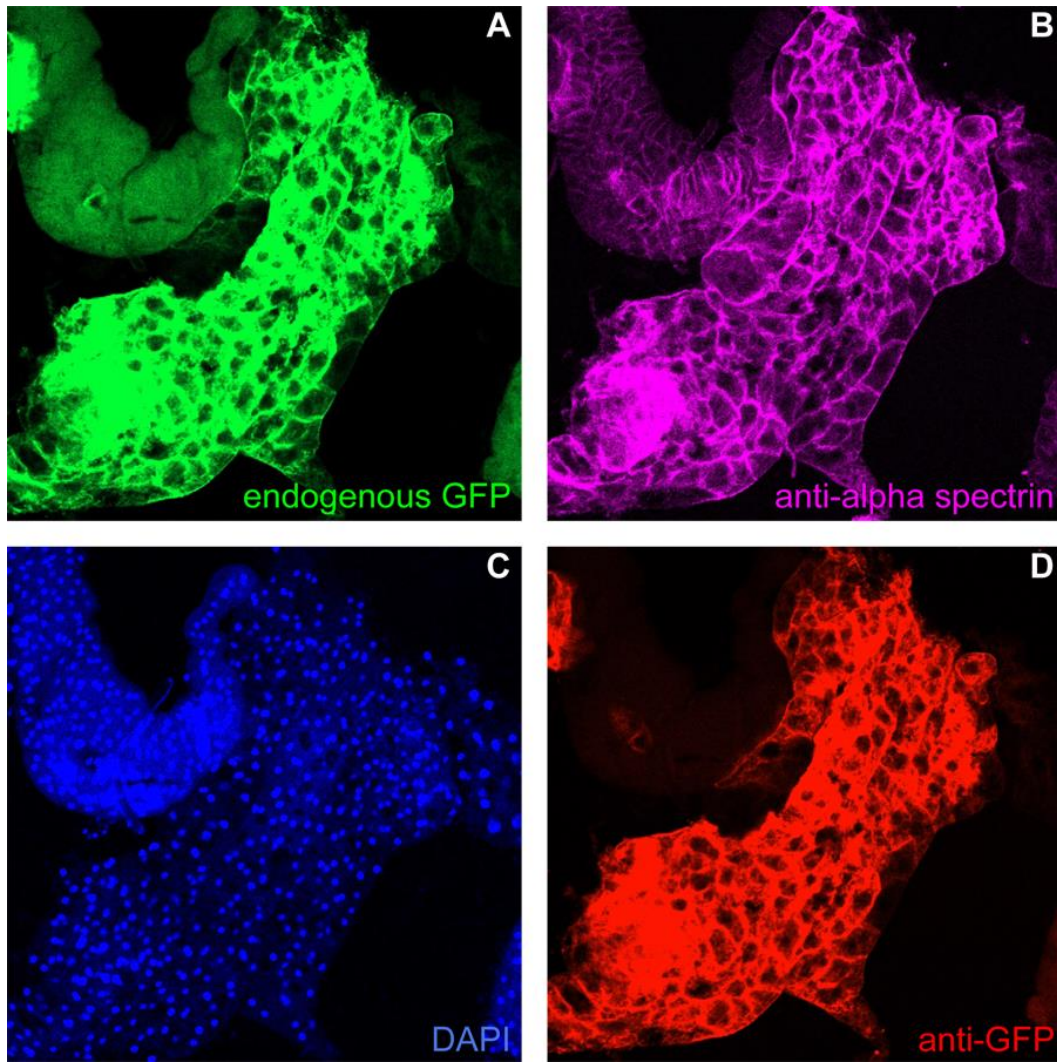


Figure 3.1 *tubP-Gal80ts; 3.1Lsp2-Gal4/TM6b > w\**; *P{10XUAS-mCD8::GFP}attP2*: (A). Endogenous GFP (B). Anti-alpha spectrin labels, cell membrane. (C) Anti-GFP, labels endogenous GFP. (D). DAPI labels nuclei.



### 3.2 PPL-GAL4 DRIVES MODERATE GENE EXPRESSION IN ADULT FAT

*w\**; *P{ppl-GAL4.P}2* is a transgenic line with the *Gal4* insertion also located on the second chromosome. This driver line is under control of the *ppl* (*pumpless*) promoter, which has been reported to encode a protein that mediates food intake suppression in response to amino acid and glycine catabolism (Zinke et al.1999). Like the *Lsp2(3.1)* insertion, *ppl-Gal4* has also been used to manipulate gene expression in the adult fat body, but it also drives in the gut and Malpighian tubules (Zaidman-Rémy et al. 2006).

As expected, when crossed with *UAS-MCD8::GFP*, *ppl-Gal4* shows strong expression in the adult fat body (See Figure 3.2). As with *Lsp2(3.1)*, this driver shows high and evenly distributed GFP signal around the cell membrane. Individual cells do have a high variation in shape and size that does not correlate with the intensity of GFP expression. In comparison with *Lsp2(3.1)*, there have been fewer cases as well as number of cells were patches of adipocytes have little to no expression.

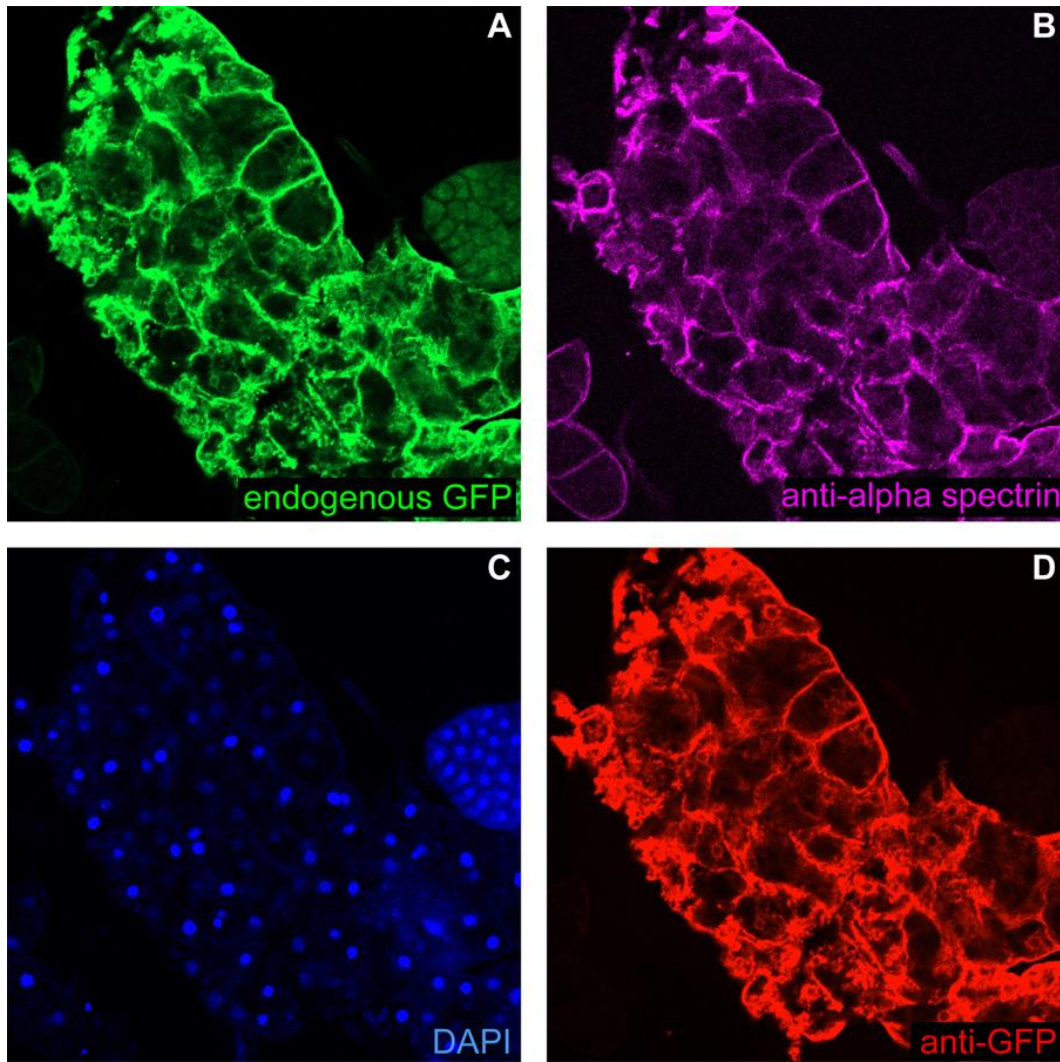


Figure 3.2  $w^*$ ;  $P\{ppl-GAL4.P\}2 > w^*$ ;  $P\{10XUAS-mCD8::GFP\}attP2$ : (A). Endogenous GFP (B). Anti-alpha spectrin labels, cell membrane. (C) Anti-GFP, labels endogenous GFP. (D). DAPI labels nuclei.

### 3.3 *C564-GAL4* DRIVES MODERATE GENE EXPRESSION IN ADULT FAT

This fly line is the first of the nine to be an enhancer detector. While similar to the previous driver lines tested, the genomic sequence that controls the expression of *Gal4* is an enhancer element, rather than a promoter sequence for a specific gene (Wilson et al. 1989). Enhancers are analogous to promoters, in that they regulate gene transcription, however the enhancer element is not directly downstream or upstream of the target gene that it actively regulates (Jin et al. 2011).  $w^{1118}$ ;  $P\{Gawb\}c564$  is located on the second chromosome and has been reported to drive expression in many tissues, including the salivary glands, male reproductive system, hemocytes, and the adult fat body (Harrison et al. 1995; Hrdlicka et al. 2002; Paredes et al. 2011).

It was seen that *c564-Gal4* drives expression in the adult fat body; however, the intensity of the expression is reduced in comparison to *ppl-Gal4* and *Lsp2(3.1)-Gal4*. The distribution of the adipocytes that do have a positive signal is even, however there are more instances where adipocytes have little to no expression especially in larger patches (see figure 3.3).

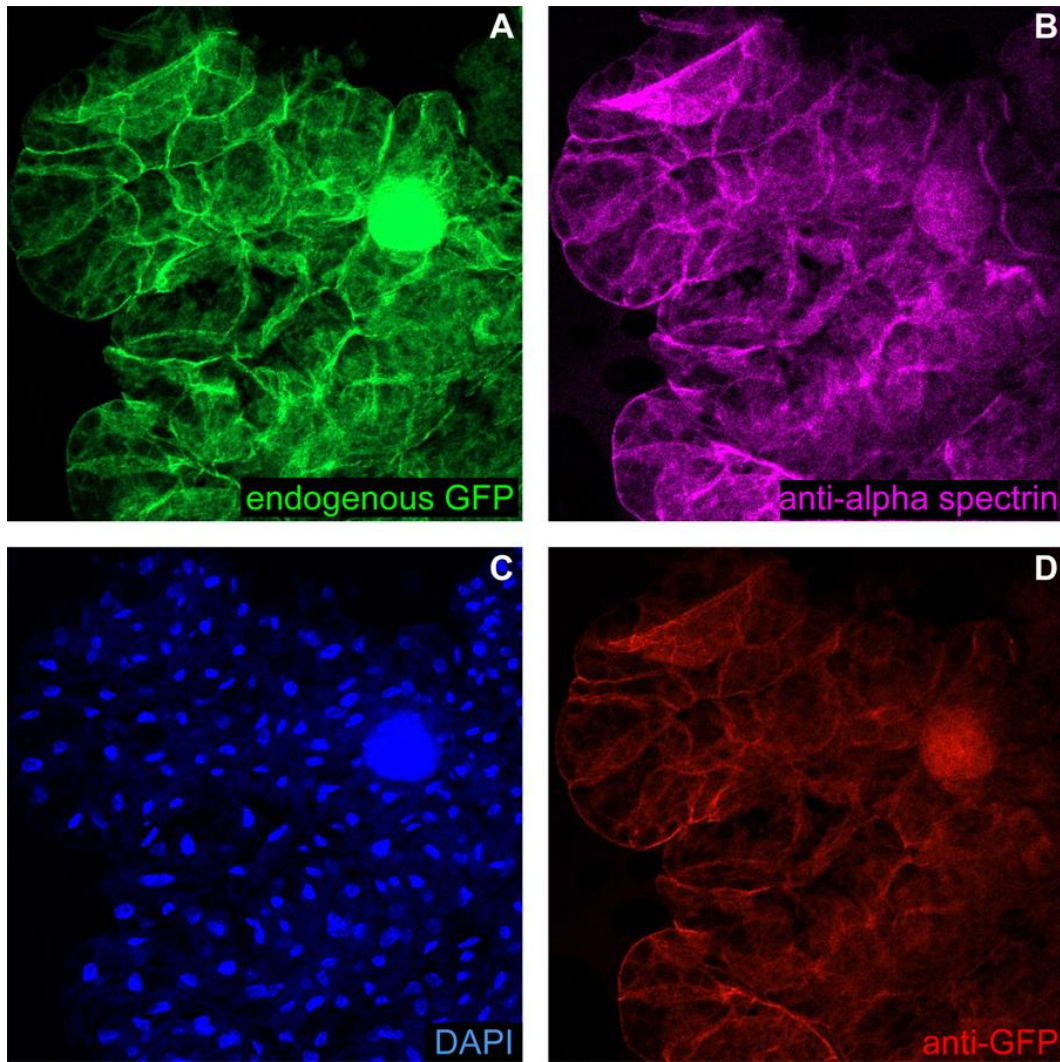


Figure 3.3  $w^{118}; P\{GawB\}c564 > w^*$ ;  $P\{10XUAS-mCD8::GFP\}attP2$ : (A). Endogenous GFP (B). Anti-alpha spectrin labels, cell membrane. (C) Anti-GFP, labels endogenous GFP. (D). DAPI labels nuclei.

### 3.4 *C754-GAL4* DRIVES LOW GENE EXPRESSION IN ADULT FAT

*P{GawB}c754, w<sup>1118</sup>* is an enhancer detector line located on the first (X) chromosome. This line has only been reported to drive expression in the adult optic lobe and select larval tissues, such as the digestive system, fat body, imaginal discs, lymph gland, and salivary gland (Harrison et al. 1995; Hrdlicka et al. 2002). In this experiment it was shown that *c754-Gal4* drives expression in the adult fat body.

While the previous enhancer line showed a decreased level of fluorescence with respect to *ppl-Gal4* and *Lsp2(3.1)-Gal4*, *c754-Gal4* appeared to have a more drastic decrease in fluorescence. The adipocytes that have a GFP signal are faint in intensity and are dispersed unevenly around the patches (see figure 3.4). In most cases there are more patches of adipocytes that have no GFP expression compared to adipocytes that do. However, regardless of the sparseness of individual cells that express GFP, nearly all patches observed have them, suggesting that *P{GawB}c754, w<sup>1118</sup>* is an abled driver of gene expression in the adult fat body.

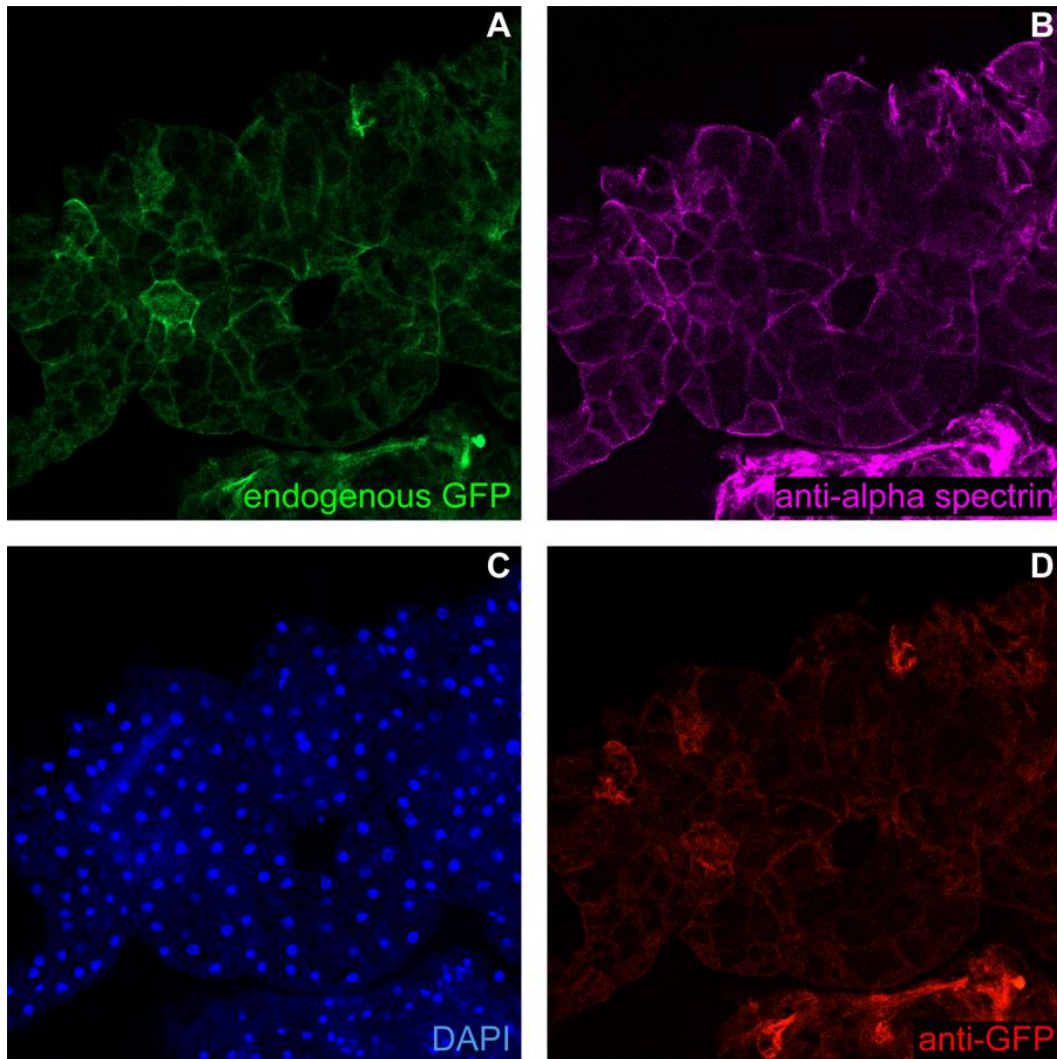


Figure 3.4  $P\{GawB\}c754, w^{1118} > w^*$ ;  $P\{10XUAS-mCD8::GFP\}attP2$ : (A). Endogenous GFP (B). Anti-alpha spectrin labels, cell membrane. (C) Anti-GFP, labels endogenous GFP. (D). DAPI labels nuclei.

### 3.5 FIVE *GAL4* LINES DID NOT DRIVE EXPRESSION IN THE ADULT FAT BODY

$y^l w^{1118}; P\{Lsp2-GAL4.H\}3$  is a driver line with the *Gal4* insertion located on the third chromosome. As with *Lsp2(3.1)-Gal4*, the promoter that controls *Gal4* expression is *Lsp2*. This fly line was originally reported to drive expression in the larval fat body however, it has been reported to drive in the adult fat body as well (Cherbas et al.2003; Takeuchi et al. 2015).

In this study, when  $y^l w^{1118}; P\{Lsp2-GAL4.H\}3$  was crossed with *UAS-MCD8::GFP*, the progeny do not show driven gene expression (see figure 3.5.1). This is apparent for all patches of adipocytes observed across multiple experiments. These findings are supported by anti-GFP staining.

After examining the previous study that reported expression in the adult tissue more thoroughly, the specific fly line and the blueprint of the constructed insertion are not stated. (Takeuchi et al. 2015). Thus, it can be assumed that the fly line used in that study was not  $y^l w^{1118}; P\{Lsp2-GAL4.H\}3$ . Additionally,  $y^l w^{1118}; P\{Lsp2-GAL4.H\}3$  could have been constructed with a modified *Lsp2* promoter fragment. In the previous study that constructed the adult specific *Lsp2(3.1)* line, a second line was constructed with the *lsp2* fragment the size 0.38 Kb (Lazareva et al. 2007). This specific promoter is only active during the larval stage (Lazareva et al. 2007). Therefore, if  $y^l w^{1118}; P\{Lsp2-GAL4.H\}3$  was constructed with the 0.38 kb fragment, then it could not have driven expression in the adult fat body.

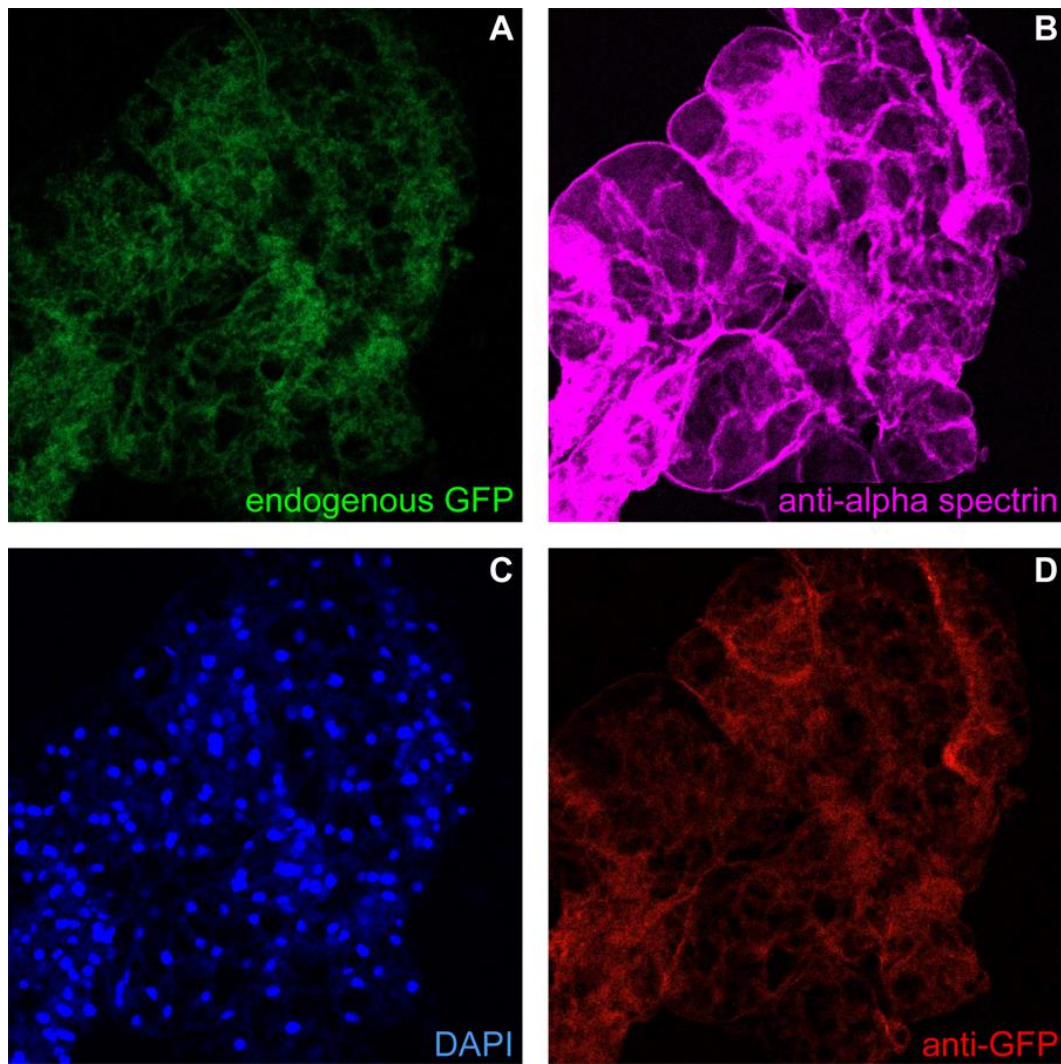


Figure 3.5 *y1 w<sup>1118</sup>; P{Lsp2-GAL4.H}3 > w\*; P{10XUAS-mCD8::GFP}attP2:*  
 (A). Endogenous GFP (B). Anti-alpha spectrin labels, cell membrane. (C)  
 Anti-GFP, labels endogenous GFP. (D). DAPI labels nuclei.



$w^{1118}; P\{GawB\}C833$  and  $w^{1118}; P\{GawB\}C855a$  are both enhancer detector lines located on the third chromosome. Both of are known to drive expression in the embryonic and larval nervous system, as well as the larval fat body, wing disc, thoracic disc, and eye disc (Hrdlicka et al. 2002; Wang et al., 2011). Additionally, both have been reported to drive expression in in the adult male reproductive system, with  $w^{1118}; P\{GawB\}C855a$  driving in the follicle cells of adult females as well (Hrdlicka et al. 2002; Susic-Jung et al., 2012).

$w^*$ ;  $P\{GawB\}c591$  and  $w^{1118}; P\{GawB\}l(2)T76T76/CyO$  are enhancer detector lines located on the second chromosome. Both fly lines have been reported to drive expression in the larval fat body, imaginal disc, salivary glands, trachea, and digestive system (Harrison et al.1995). Additionally,  $w^{1118}; P\{GawB\}l(2)T76T76/CyO$  drives expression in the adult male reproductive system (Hrdlicka et al. 2002).

The findings of this this study found, that when these four lines were crossed with  $UAS-MCD8::GFP$ , that they do not drive expression in the adult fat body. Individual adipocytes, in addition to patches of adipocytes, had no GFP signal. These results are supported by anti-GFP Staining (See Figures 3.6 -3.9).

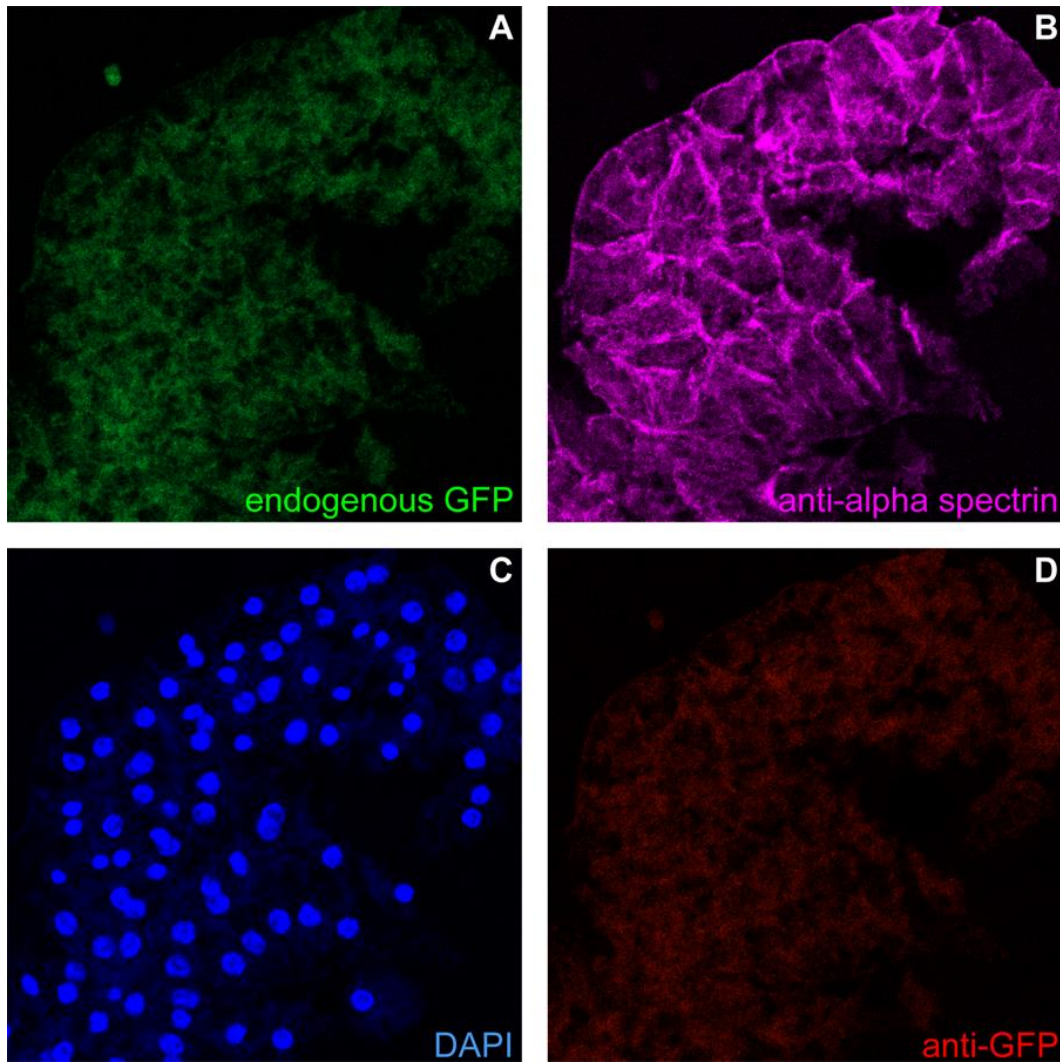


Figure 3.6  $w^{1118}; P\{GawB\}C833 > w^*$ ;  $P\{10XUAS-mCD8::GFP\}attP2$ : (A). Endogenous GFP (B). Anti-alpha spectrin labels, cell membrane. (C) Anti-GFP, labels endogenous GFP. (D). DAPI labels nuclei.

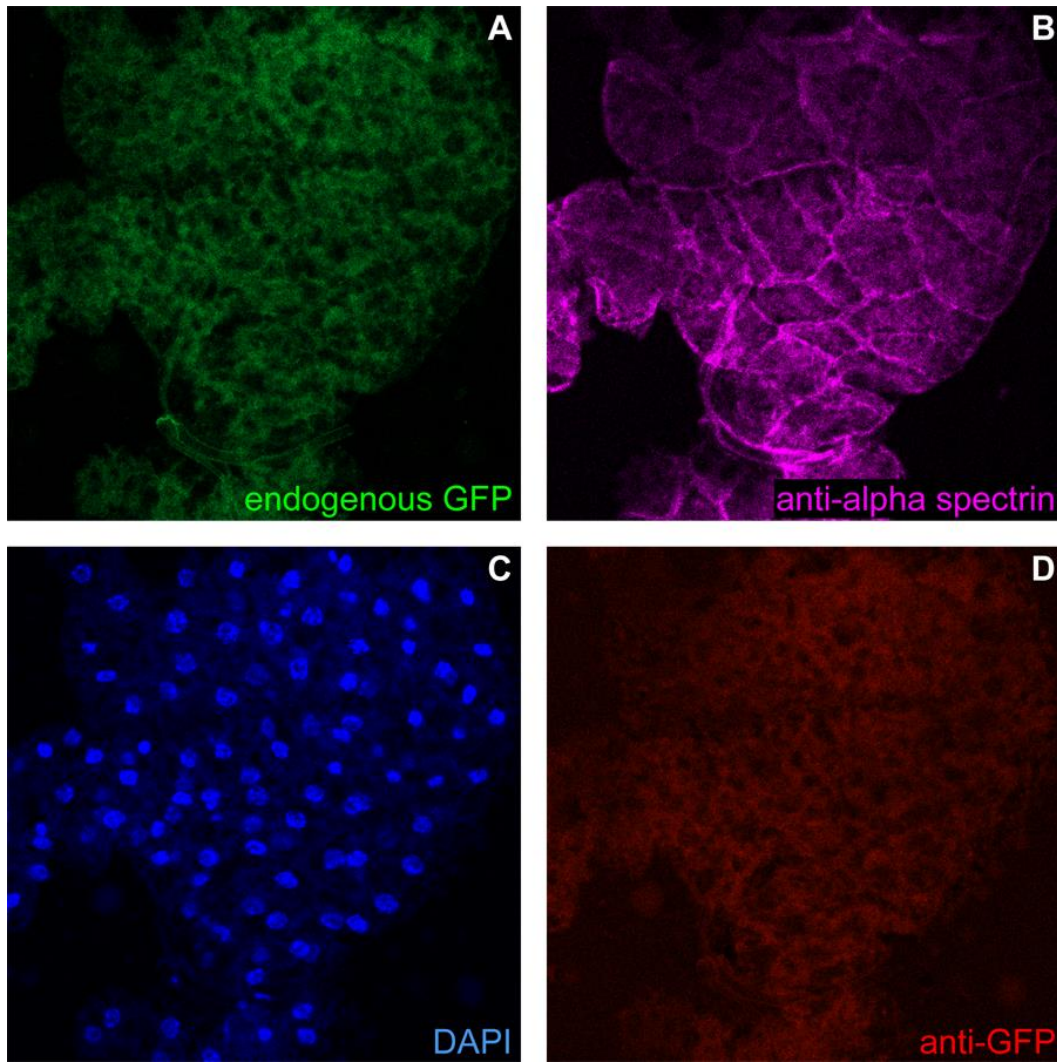


Figure 3.7  $w^{1118}; P\{GawB\}C855a > w^*$ ;  $P\{10XUAS-mCD8::GFP\}attP2$ : (A). Endogenous GFP (B). Anti-alpha spectrin labels, cell membrane. (C) Anti-GFP, labels endogenous GFP. (D). DAPI labels nuclei.

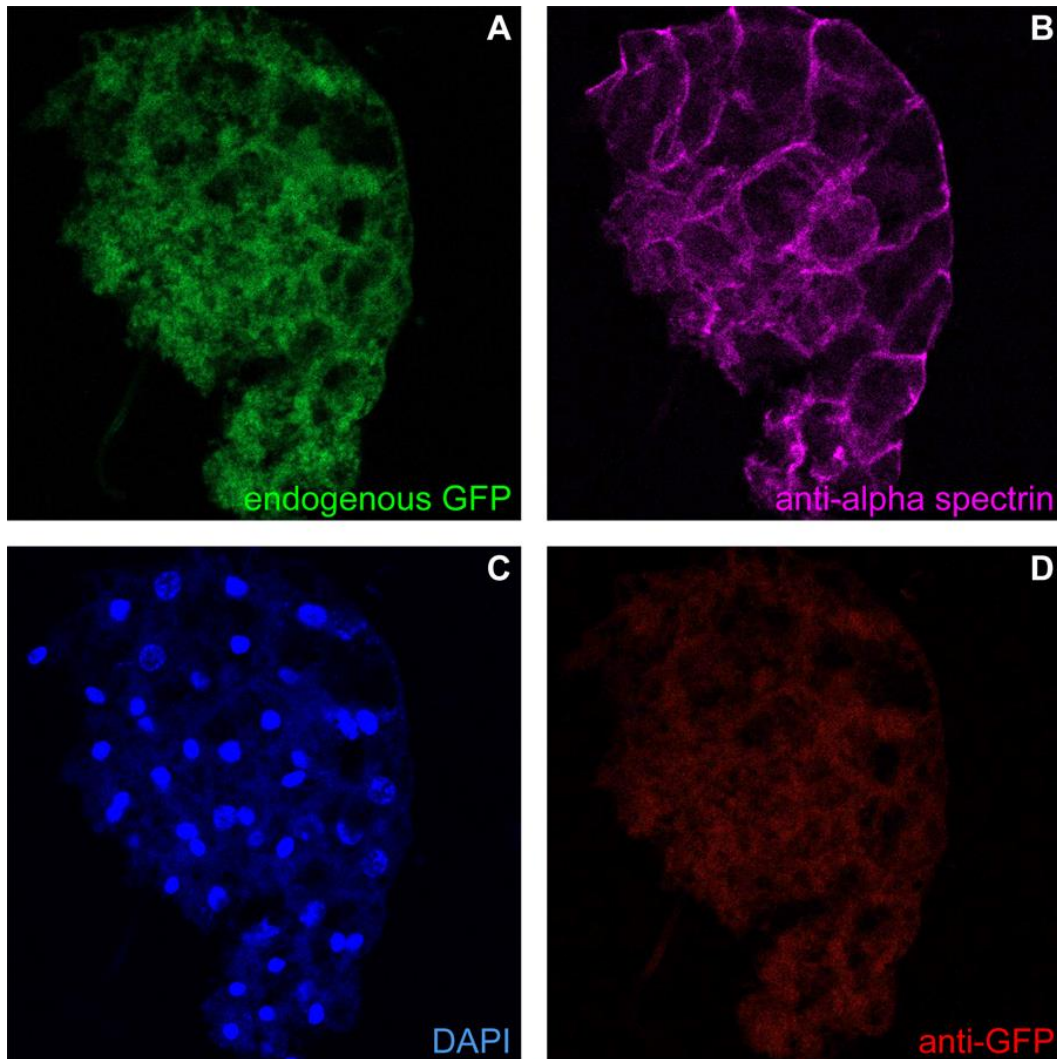


Figure 3.8  $w^*$ ;  $P\{GawB\}c591 > w^*$ ;  $P\{10XUAS-mCD8::GFP\}attP2$ : (A). Endogenous GFP (B). Anti-alpha spectrin labels, cell membrane. (C) Anti-GFP, labels endogenous GFP. (D). DAPI labels nuclei..

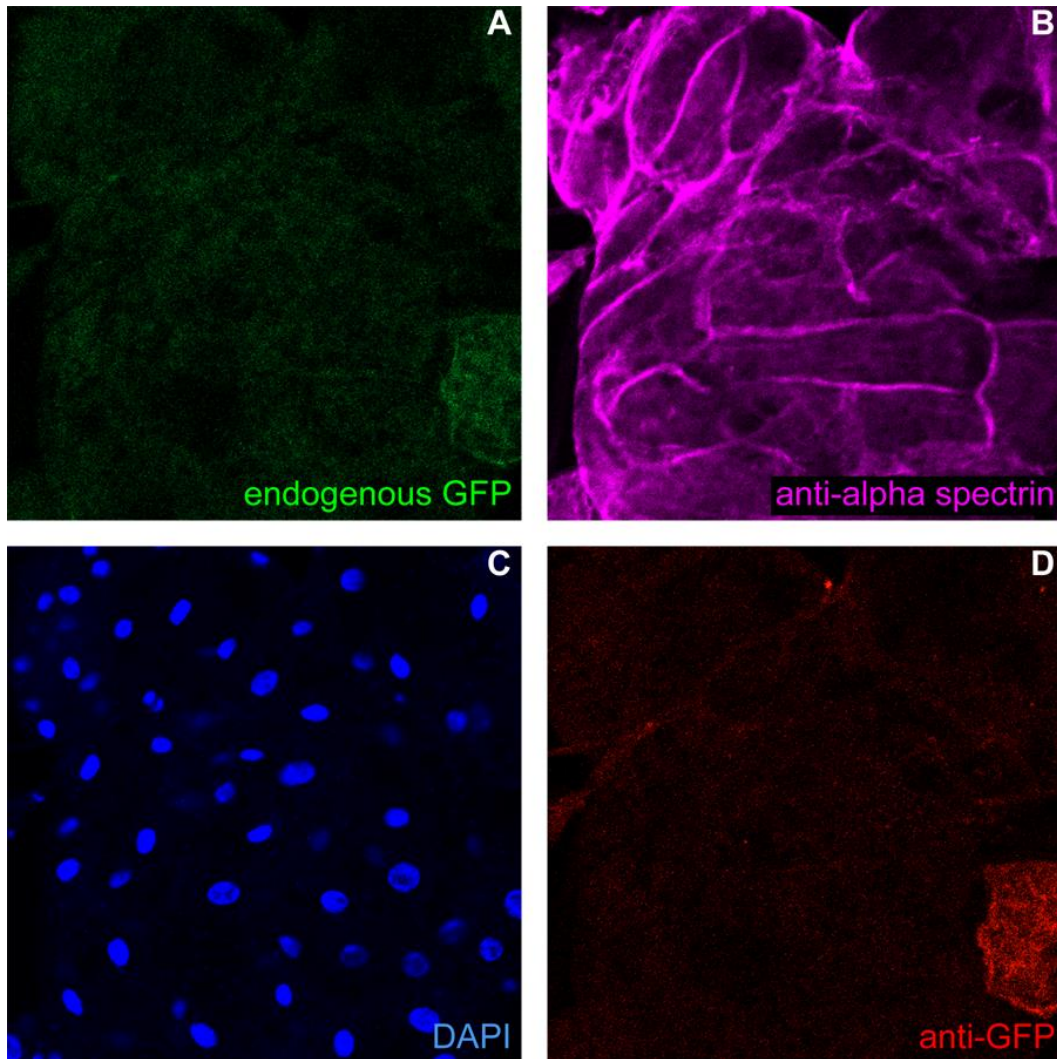


Figure 3.9  $w^{1118}; P\{GawB\}l(2)T76T76/CyO > w^*$ ;  $P\{10XUAS-mCD8::GFP\}attP2$ : (A). Endogenous GFP (B). Anti-alpha spectrin labels, cell membrane. (C) Anti-GFP, labels endogenous GFP. (D). DAPI labels nuclei.

## CHAPTER 4

### GENE EXPRESSION AND CELL MORPHOLOGY

#### 4.1 COMPARISON OF GENE EXPRESSION OF ADULT FAT BODY DRIVERS

Four out of the nine driver lines tested, drove expression in the adult fat body. Three out of those four lines were re-evaluated to quantify the relative level gene expression with respect to  $w^{1118}$ . The  $w^{1118}$  fly line does not have a *Gal 4* insertion and thus serve as a negative control to gauge transgene expression. The three lines of interest were *tubP-Gal80<sup>ts</sup>*; *3.1Lsp2-Gal4/TM6b, w\**; *P{ppl-GAL4.P}2*, and *P{GawB}c754, w<sup>1118</sup>*. The former two lines had high uniform GFP fluorescence and were previously reported to drive expression in the adult tissues, while the latter had qualitatively low GFP fluorescence, and has not been previously reported to drive expression in the adult tissues.

To quantify the level of gene expression, individual adipocytes had their perimeter traced. The average GFP intensity was calculated based on the pixel intensity of the area of the drawn shape. These values were summed, and the means were calculated between the genotypes. *Lsp2(3.1) > MCD8* had the highest GFP intensity of the tested lines, while *ppl-Gal > MCD8* and *c754 > MCD8* had comparatively higher GFP intensity with respect to the control (see figure 4.1). Through an ANOVA, it was found that there was a significant difference between the GFP intensities among the genotypes ( $F(3, 670) = 124.1$ ) (see figure 4.1). In order to examine the pairwise differences between GFP intensity among each individual genotype, a post-hoc Tukey's

range test was performed. It was found that there was not significant difference between *ppl-Gal* > *MCD8* and *c754* > *MCD8* ( $P = 0.9755$ ), however there was a significant difference between the comparison of each other genotype (see figure 4.2). This data indicates that there is a measurable difference between transgene expression among the genotypes.

## Average GFP vs Genotype

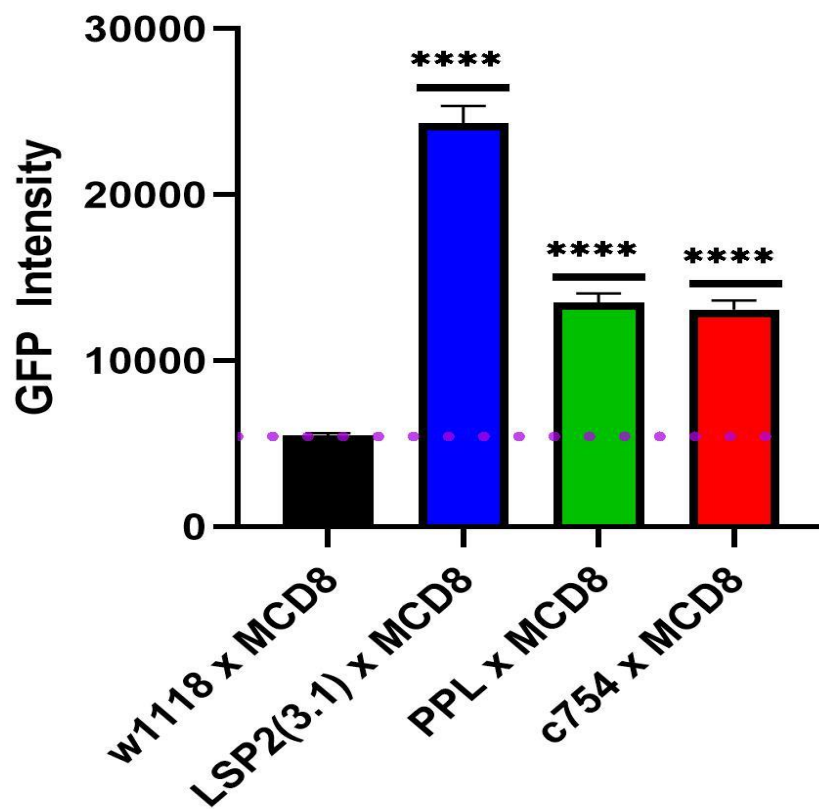


Figure 4.1 Average GFP intensity of each individual cross: GFP signal was measured by pixel intensity of the defined drawn area. N = 147,176, 229, 122. ANOVA analysis:  $F(3, 670) = 124.1$ ,  $P < 0.0001$ . Asterisks represent statistical significance with respect



### 95% Confidence Intervals (Tukey)

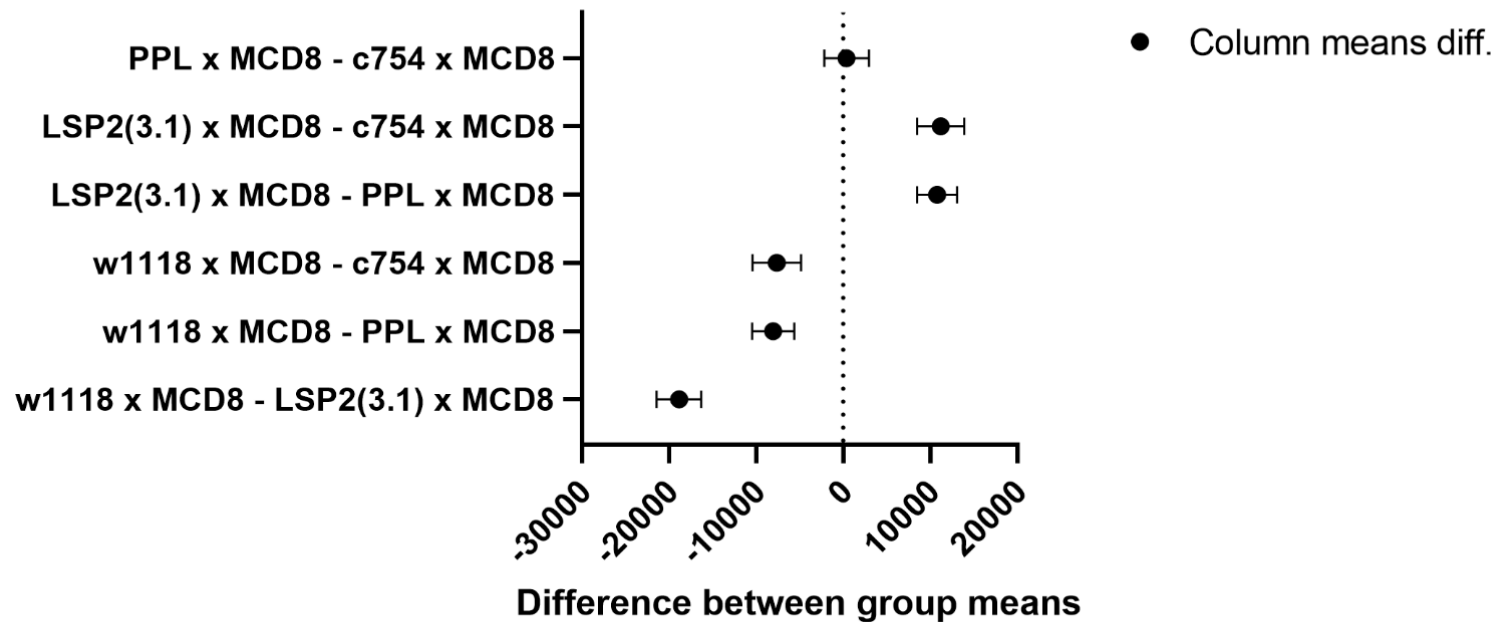


Figure 4.2 Tukey's range test between genotypes 1: In addition to comparison with the negative control cross, tests were performed between each experimental cross as well. There was a significant difference between *LSP2(3.1)* > *MCD8* and *c754* > *MCD8* ( $P < 0.0001$ ), and *LSP2(3.1)* > *MCD8* and *PPL* > *MCD8* ( $P < 0.0001$ ). There was not a significant difference between *PPL* > *MCD8* and *c754* > *MCD8* ( $P < 0.9755$ ).

## 4.2 GENE EXPRESSION WITH RESPECT TO CELL SIZE

As stated previously, there have been reported morphological differences in the fat body of other insects. (Haunerland and Shirk 1995). However, there is also variation in adipose tissue seen in mammals, for example, adipocytes in mammals are divided between brown and white adipocytes (Saely et al. 2012; Rosell et al. 2014). Brown adipocytes have smaller lipid droplets, a higher number of mitochondria, and a different function compared to white adipocytes (Saely et al. 2012). To identify if there are similar characteristics applicable to the adult *Drosophila* fat body, the GFP intensity was measured in conjunction with cell membrane size.

Cell size was measured by utilizing the anti-alpha-spectrin staining as the outline of the cell membrane. GFP intensity was again calculated by measuring the pixel intensity of the defined drawn adipocyte. This information was then acquired for each genotype; plotting each individual adipocyte with its respective GFP intensity and size. In comparison with the  $w^{1118}$  control, there was negative correlation between GFP intensity and cell membrane size for  $Lsp2(3.1) > MCD8$  and  $c754 > MCD8$ . (see figure 4.3 and 4.5).  $Ppl > MCD8$  had a positive correlation between GFP intensity and cell membrane size with respect to the control (see figure 4.4).

Linear regressions were run on each individual genotype plot, to elucidate if cell membrane size is an adequate predictor of gene expression. For each genotype, the  $R^2$  value for each regression was less than 15%, indicating that cell size explained a relatively small, but still significant, amount of the variance in gene expression. The regressions for each genotype were statistically significant, supporting that increasing cell size is associated with increased promoter activity in the case for  $Ppl \times MCD8$  and

decreasing cell size is associated with increased promoter/enhancer activity for *Lsp2*(3.1)

> *MCD8* and to a lesser extent *c754* > *MCD8* (see figures 4.3-4.6).

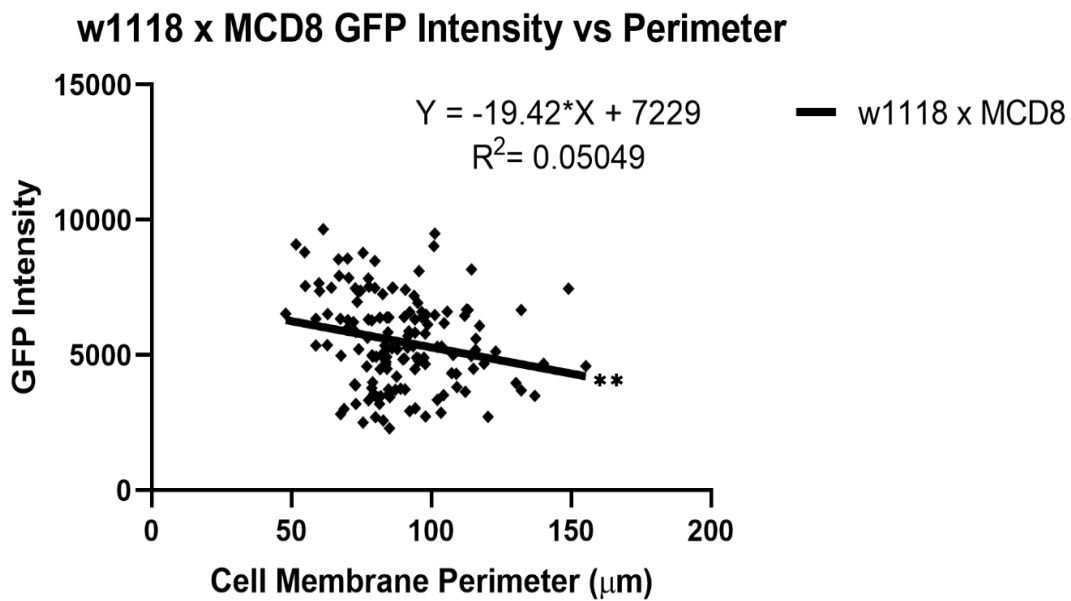


Figure 4.3  $w^{1118} > UAS-mCD8::GFP$  GFP intensity vs perimeter: Fluorescence analysis has minor background signal with respect to negative control. For the linear regression  $F(1, 145) = 7.710$ ,  $P = 0.0062$ .

### LSP2(3.1) x MCD8 GFP Intensity vs Perimeter

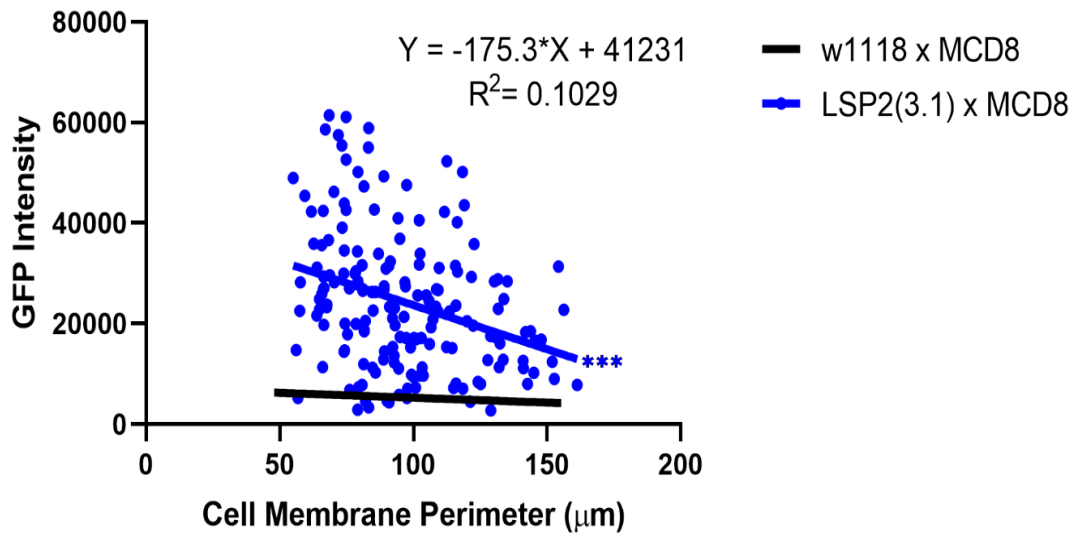


Figure 4.4 *Lsp2(3.1)-GAL4 >x UAS-mCD8::GFP* GFP intensity vs perimeter: GFP intensity decreases as cell size increases in relation to the control. For the linear regression,  $F(1, 174) = 19.97$ ,  $P < 0.0001$ .

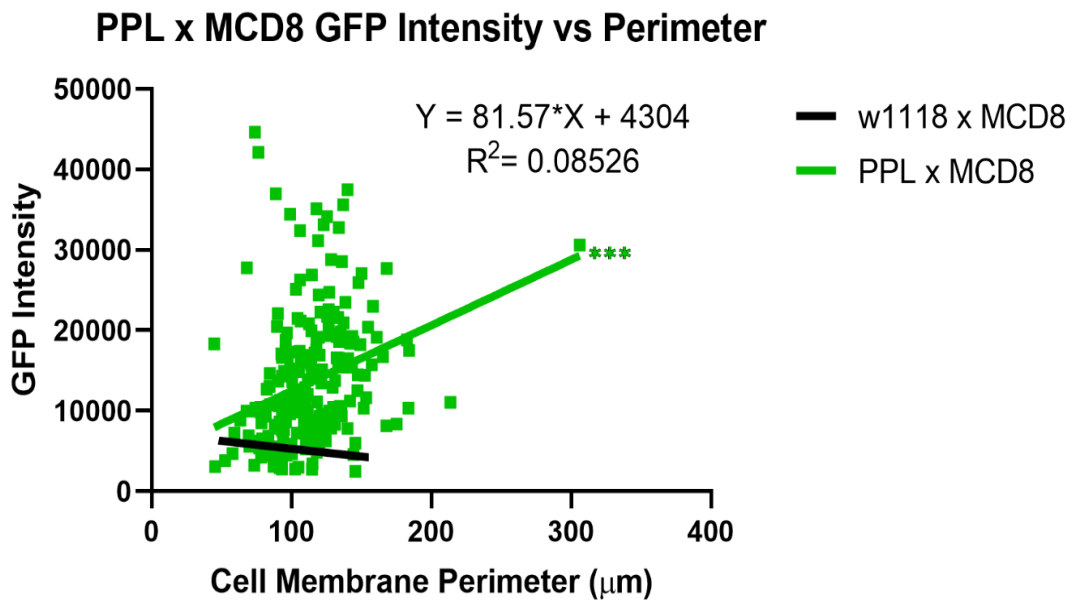


Figure 4.5 *PPL-GAL4 > UAS-mCD8::GFP* GFP intensity vs perimeter: GFP intensity increases as cell size increases in relation to the control. For the linear regression,  $F(1,227) = 21.16$ ,  $P < 0.0001$ .

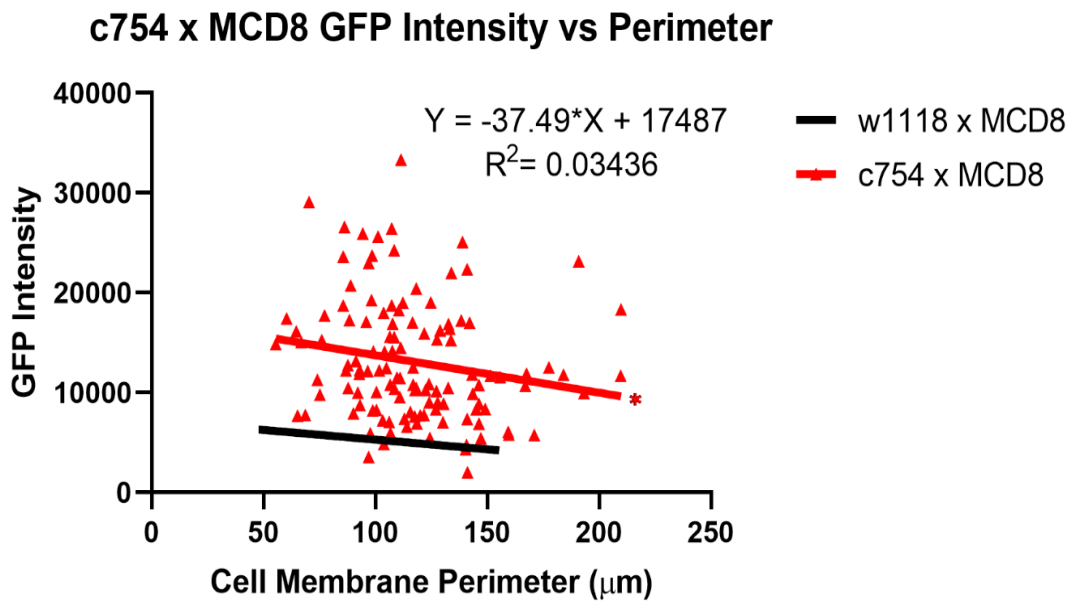


Figure 4.6 *c754-GAL4 > UAS-mCD8::GFP* GFP intensity vs perimeter: GFP intensity has a minor decrease as cell size increases in relation to the control.  $F(1,120) = 4.270$ ,  $P = 0.0409$ .

### 4.3 COMPARING REGRESSIONS AMONG TRANSGENIC DRIVER LINES

The previous data indicates that there is a relationship between cell size and the level of gene expression. In order to compare that relationship between transgenic lines, an analysis was performed to compare the slopes of each regression (see figure 4.7). An ANOVA was run using the expression level over the cell size (the slope) for each regression as the dependent variable and the genotype as the independent variable (see figure 4.7). Additionally, a Tukey's post hoc test was performed to compare each genotype individually (see figure 4.8). The ANOVA indicated that the slopes of the regressions were significantly different ( $F(3, 666) = 21.11$ ) (see figure 4.7) but, individually the relationship between the slopes differed depending on the genotypes compared. *Lsp2(3.1) > MCD8* and *ppl > MCD8* had a significant difference in comparison with the control ( $P < 0.0001$  and  $P < 0.0167$ ) (see figure 4.8). However, the slope of *c754 > MCD8* was not found to be significantly different in comparison with the control ( $P < 0.9683$ ) but was found to be significantly different in comparison with the other two genotypes ( $P < 0.0018$  and  $P < 0.0058$ ) (see figure 4.8).

This data indicates that the relationship between cellular size on gene expression is modulated based on the gene of interest. In the case of this study, larger adipocytes will have increased levels *ppl* activity, decreased *lsp2* activity, and relatively unchanged activity of the *c754* enhancer.



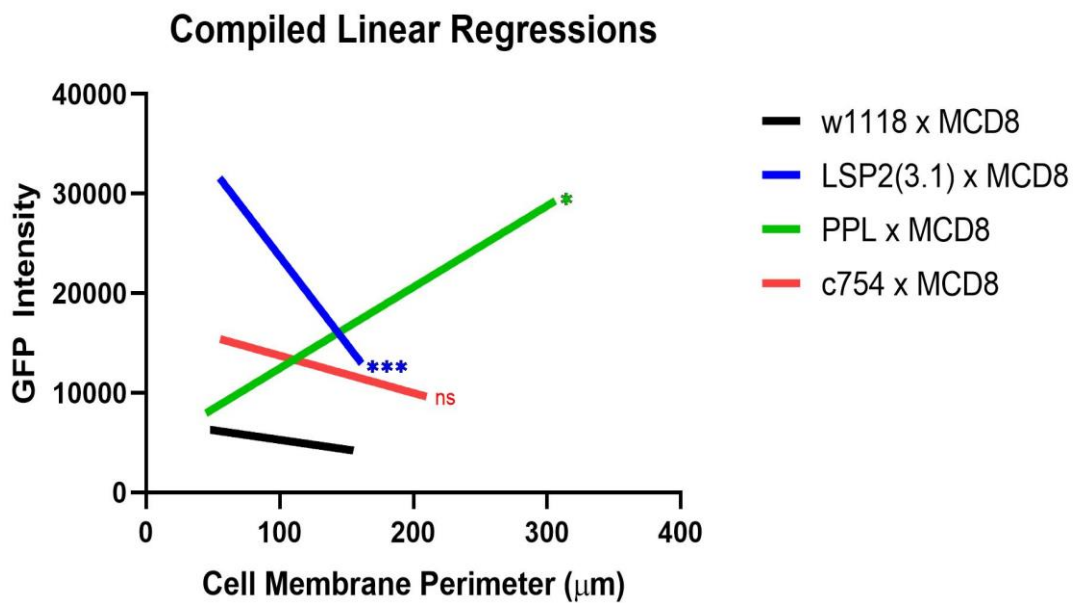


Figure 4.7 Compiled regressions of each individual cross: The slopes of each regression were utilized as the dependent variable. ANOVA analysis:  $F(3, 666) = 21.11$ . Asterisks represent statistical significance with respect to the control via Tukey's Range test. *Lsp2(3.1) x MCD8* and *ppl x MCD8* were significant different with respect to the control,  $P < 0.0001$  and  $P = 0.0167$ . *c754 x MCD8* was not found to be significantly different with *w<sup>1118</sup>*,  $P = 0.9683$

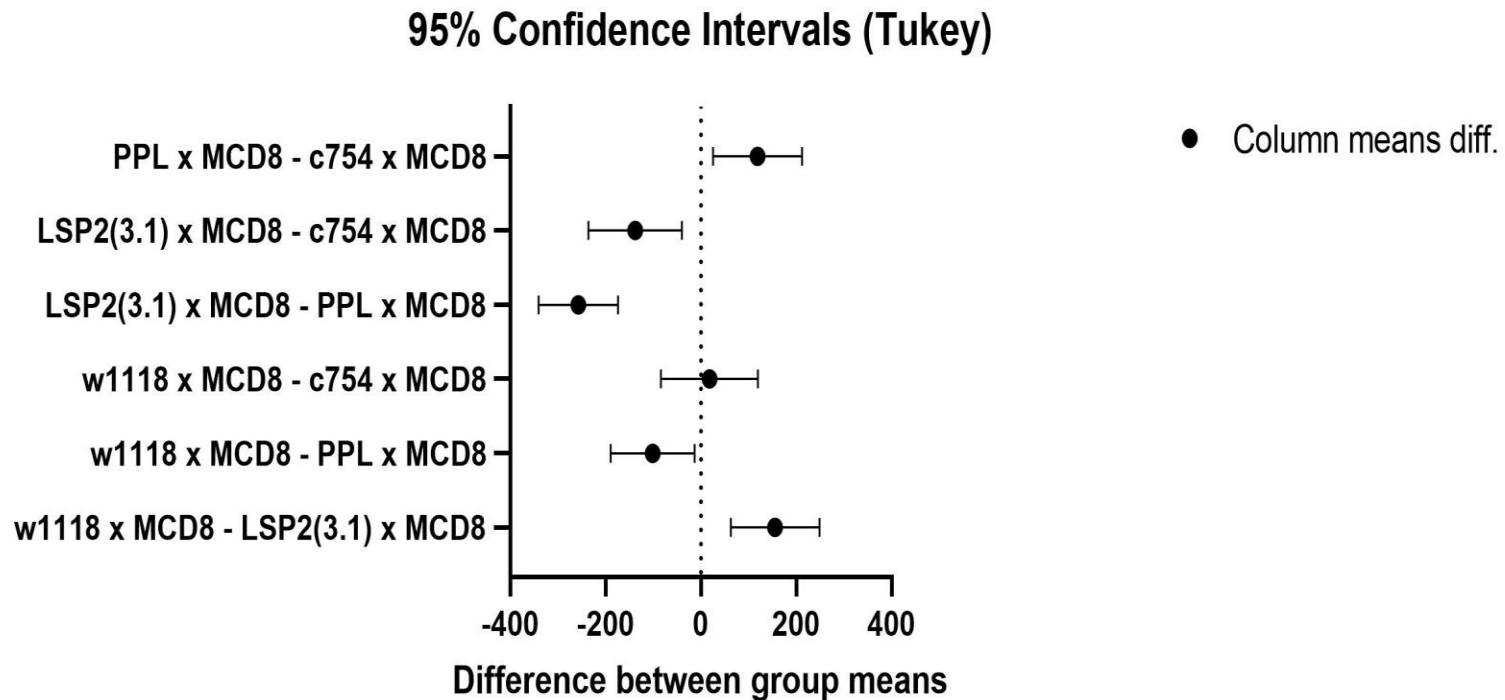


Figure 4.8 Tukey's range test between genotypes 2: In addition to comparison with the negative control cross, tests were performed between each experimental cross as well. There was a significant difference between *PPL x MCD8* and *c754 x MCD8* ( $P = 0.0058$ ), *LSP2(3.1) x MCD8* and *c754 x MCD8* ( $P = 0.0018$ ), and *LSP2(3.1) x MCD8* and *PPL x MCD8* ( $P < 0.0001$ ).

## CHAPTER 5

### DISCUSSION

The results of this study revealed that four out of the nine *Gal4* lines tested positive to promote gene expression in the adult fat body. Of these four *Gal4* lines, one was not previously reported to do so; thus, revealing an additional genetic tool to study the adult tissue. This line was characterized by a weaker GFP intensity with respect to the other positive fat body drivers (see figure 3.4). In addition, the adipocytes that do promote driven expression were dispersed throughout the tissue (see figure 3.4).

This difference in expression could be useful in a variety of different studies. For example, a study utilizing RNAi decreased basal levels of gene expression and helped elucidate the functionality of genes *frizzled* and *frizzled 2* (Kennerdell and Carthew 1998). Utilizing a defined *UAS-RNAi* line, and in addition *Lsp2(3.1)-Gal 4*, and *c754-Gal4*, a study could be performed to measure the effects of disrupted gene expression at different magnitudes in a fat body specific manner.

In trying to uncover if there was relationship between gene expression and cell morphology, it was found that there was discernable link between GFP intensity and cell membrane size among the genotypes. The correlational relationship for both *Lsp2(3.1) > MCD8* and *c754 > MCD8* was negative, while positive for *ppl > MCD8* (see figures 4.3 - 4.6). This correlational relationship was then expanded further through regression analysis, indicating that there was a significant relationship between cell size on the level of gene expression, between each genotype (see figure 4.3-4.6). These

significant relationships between individual genotypes, were then compared by using the slopes of each regression. It was found that there was a significant difference among all the genotypes with respect to the relationship between GFP intensity and cell size (see figure 4.7). This significance was confirmed additionally by comparing each genotype's slope with one another (see figure 4.8). This information altogether supports that cellular size is related to the level of activity of promoters for specific genes in adult adipocytes.

There are additional morphological parameters that differ among sub-cell populations that could be applied to the adult fat body. As previously stated, brown fat and white fat in mammals differs in organelle composition, with white fat having less mitochondria compared to brown; this leads to a difference in functionality between the two sub-cell types (Cedikova et al 2016). Immunostaining specific organelles has been used to study cell characteristics in many tissues, for example, a previous study used mitochondria fluorophores to observe the effects of a cyclin dependent protein kinase complex on mitochondria activity in the larval fat body of *Drosophila* (Frei et al. 2005). Utilizing organelle fluorophores, further morphological differentiation can be made in the fat body of the adult *Drosophila* as well.

In addition to morphological features, different anatomical populations could be studied too. Recent studies have indicated, that there is a difference of gene expression between the adult fat body of the head and the adult fat body of the abdomen and this difference is affected by high fat diet (Stobdan et al. 2019). Additionally, as previously stated, there has been a difference in gene expression among these fat body populations, which has affected other tissues by modulating insulin signaling (Hwangbo

et al 2004). Therefore, expanding this study's focus to both the head and thoracic fat might be a necessity in the future.

There are 25 publicly available *Gal4* lines that are reported to drive expression in the larval fat body and in this study, it was confirmed that one of those lines does drive expression in the adult tissue and four of those lines do not. Thus, there are 20 lines that have not been reported to drive expression which still need to be tested. Confirming if these lines drive expression in the adult fat body would provide a more robust set of tools for studying the tissue itself.

Additionally, many techniques have been developed to study the organs system of *Drosophila* on an organismal scale such as tissue clearing and belly mount imaging. The first method utilizes a specific chemical cocktail to remove the pigmentation of the *Drosophila* exo-skeleton, which allows for visualization of the internal tissues without the need for dissection. (Pendes et al. 2018). The second method utilizes a modified cover slip and microscope slide system in tandem with a clear adhesive. This allows for intact confocal imaging of the anatomical regions of interest (Koyama et al 2019). Future, experiments will need to incorporate these techniques in combination with the aforementioned immunostaining of organelles, to elucidate if there are discernable differences among adipocytes.

The characterization of adipocytes of the adult *Drosophila* fat body will lead to a better understanding of the tissue's role in interorgan communication. If these future studies confirm that there is a subpopulation of adipocytes that are morphologically distinguishable and reveal the specific *Gal4* line that is associated with them, then a functional analysis can be performed to distinguish them further. A difference in

functionality could indicate a division between cellular communication, and therefore affect other systems if ablated. By utilizing *UAS-rpr*, a transgenic line, which promotes the synthesis of a pro-apoptotic factor, these specific adipocytes can be targeted for death (Ryo et al. 2002). Once genetically ablated, the effects organismal survival as well as the effects on other tissues, such as the *Drosophila* stem cell supported ovary, can be studied. This would lead to a better understanding of that cell subpopulation's role in communicating with other systems and thus their overall role in organismal homeostasis.

## REFERENCES

- Armstrong, A. R. and Drummond-Barbosa, D.** (2018). Insulin signaling acts in adult adipocytes via GSK-3 $\beta$  and independently of FOXO to control *Drosophila* female germline stem cell numbers. *Developmental Biology* **440**, 31–39.
- Armstrong, A. R., Laws, K. M. and Drummond-Barbosa, D.** (2014). Adipocyte amino acid sensing controls adult germline stem cell number via the amino acid response pathway and independently of Target of Rapamycin signaling in *Drosophila*. *Development* **141**, 4479–4488.
- Arrese, E. L. and Soulages, J. L.** (2010). Insect Fat Body: Energy, Metabolism, and Regulation. *Annual Review of Entomology* **55**, 207–225.
- Bhavanasi, D. and Klein, P. S.** (2016). Wnt Signaling in Normal and Malignant Stem Cells. *Curr Stem Cell Rep* **2**, 379–387.
- Bieberich, E. and Wang, G.** (2013). Molecular Mechanisms Underlying Pluripotency. In *Pluripotent Stem Cells* (ed. D. Bhartiya and N. Lenk), Ch.8. London, UK: *IntechOpen*.
- Bresnick, E. H., Hewitt, K. J., Mehta, C., Keles, S., Paulson, R. F. and Johnson, K. D.** (2018). Mechanisms of erythrocyte development and regeneration: implications for regenerative medicine and beyond. *Development* **145**, dev151423.
- Brock, H. W. and Roberts, D. B.** (1980). Comparison of the Larval Serum Proteins of *Drosophila Melanogaster*. *European Journal of Biochemistry* **106**, 129–135.

- Brogiolo, W., Stocker, H., Ikeya, T., Rintelen, F., Fernandez, R. and Hafen, E.** (2001). An evolutionarily conserved function of the *Drosophila* insulin receptor and insulin-like peptides in growth control. *Current Biology* **11**, 213–221.
- Castillo-Armengol, J., Fajas, L. and Lopez-Mejia, I. C.** (2019). Inter-organ communication: a gatekeeper for metabolic health. *EMBO reports* **20**, e47903.
- Cedikova, M., Kripnerová, M., Dvorakova, J., Pitule, P., Grundmanova, M., Babuska, V., Mullerova, D. and Kuncova, J.** (2016). Mitochondria in White, Brown, and Beige Adipocytes. *Stem Cells Int* **2016**, 6067349.
- Cherbas, L., Hu, X., Zhimulev, I., Belyaeva, E. and Cherbas, P.** (2003). EcR isoforms in *Drosophila*: testing tissue-specific requirements by targeted blockade and rescue. *Development* **130**, 271–284.
- Droujinine, I. A. and Perrimon, N.** (2016). Interorgan Communication Pathways in Physiology: Focus on *Drosophila*. *Annual Review of Genetics* **50**, 539–570.
- Ford, E. S., Zhao, G., Tsai, J. and Li, C.** (2011). Low-Risk Lifestyle Behaviors and All-Cause Mortality: Findings From the National Health and Nutrition Examination Survey III Mortality Study. *Am J Public Health* **101**, 1922–1929.
- Frei, C., Galloni, M., Hafen, E. and Edgar, B. A.** (2005). The *Drosophila* mitochondrial ribosomal protein mRpL12 is required for Cyclin D/Cdk4-driven growth. *The EMBO Journal* **24**, 623–634.
- Gáliková, M. and Klepsatel, P.** (2018). Obesity and Aging in the *Drosophila* Model. *International Journal of Molecular Sciences* **19**, 1896.



- Greene, J. C., Whitworth, A. J., Kuo, I., Andrews, L. A., Feany, M. B. and Pallanck, L. J.** (2003). Mitochondrial pathology and apoptotic muscle degeneration in *Drosophila parkin* mutants. *Proc Natl Acad Sci U S A* **100**, 4078–4083.
- Hales, C. M.** (2017). Prevalence of Obesity Among Adults and Youth: United States, 2015–2016. *NCHS data brief* **288**. Hyattsville, MD: National Center for Health Statistics.
- Hales, K. G., Korey, C. A., Larracunte, A. M. and Roberts, D. M.** (2015). Genetics on the Fly: A Primer on the *Drosophila* Model System. *Genetics* **201**, 815–842.
- Harrison, D. A., Binari, R., Nahreini, T. S., Gilman, M. and Perrimon, N.** (1995). Activation of a *Drosophila* Janus kinase (JAK) causes hematopoietic neoplasia and developmental defects. *EMBO J* **14**, 2857–2865.
- Haslam, D. W. and James, W. P. T.** (2005). Obesity. *The Lancet* **366**, 1197–1209.
- Hauerland, N. H. and Shirk, P. D.** (1995). Regional and Functional Differentiation in the Insect Fat Body. *Annu. Rev. Entomol.* **40**, 121–145.
- Hrdlicka, L., Gibson, M., Kiger, A., Micchelli, C., Schober, M., Schöck, F. and Perrimon, N.** (2002). Analysis of twenty-four Gal4 lines in *Drosophila Melanogaster*. *Genesis* **34**, 51–57.
- Hwangbo, D. S., Gersham, B., Tu, M.-P., Palmer, M. and Tatar, M.** (2004). *Drosophila* dFOXO controls lifespan and regulates insulin signalling in brain and fat body. *Nature* **429**, 562–566.
- Iaquinta, M. R., Mazzoni, E., Bononi, I., Rotondo, J. C., Mazziotta, C., Montesi, M., Sprio, S., Tampieri, A., Tognon, M. and Martini, F.** (2019). Adult Stem Cells for Bone Regeneration and Repair. *Front. Cell Dev. Biol.* **7**, 268–283.

- Inaki, M., Yoshikawa, S., Thomas, J. B., Aburatani, H. and Nose, A.** (2007). Wnt4 Is a Local Repulsive Cue that Determines Synaptic Target Specificity. *Current Biology* **17**, 1574–1579.
- Jin, F., Li, Y., Ren, B. and Natarajan, R.** (2011). Enhancers. *Transcription* **2**, 226–230.
- Kennerdell, J. R. and Carthew, R. W.** (1998). Use of dsRNA-Mediated Genetic Interference to Demonstrate that frizzled and frizzled 2 Act in the Wingless Pathway. *Cell* **95**, 1017–1026.
- Koh, K., Evans, J. M., Hendricks, J. C. and Sehgal, A.** (2006). A *Drosophila* model for age-associated changes in sleep:wake cycles. *Proc Natl Acad Sci U S A* **103**, 13843–13847.
- Koyama, L. A. J., Aranda-Díaz, A., Su, Y.-H., Balachandra, S., Martin, J. L., Ludington, W. B., Huang, K. C. and O'Brien, L. E.** (2019). Bellymount enables longitudinal, intravital imaging of abdominal organs and the gut microbiota in adult *Drosophila*. *PLOS Biol* **18**(1), e3000567.
- Lazareva, A. A., Roman, G., Mattox, W., Hardin, P. E. and Dauwalder, B.** (2007). A Role for the Adult Fat Body in *Drosophila* Male Courtship Behavior. *PLOS Genetics* **3**, e16.
- Mahla, R. S.** (2016). Stem Cells Applications in Regenerative Medicine and Disease Therapeutics. *Int J Cell Biol* **2016**, 6940283.
- Makki, R., Cinnamon, E. and Gould, A. P.** (2014). The Development and Functions of Oenocytes. *Annual Review of Entomology* **59**, 405–425.

- Mihaylova, M. M., Sabatini, D. M. and Yilmaz, Ö. H.** (2014). Dietary and Metabolic Control of Stem Cell Function in Physiology and Cancer. *Cell Stem Cell* **14**, 292–305.
- Ohlhorst, S. D., Russell, R., Bier, D., Klurfeld, D. M., Li, Z., Mein, J. R., Milner, J., Ross, A. C., Stover, P. and Konopka, E.** (2013). Nutrition research to affect food and a healthy life span. *J Nutr* **143**, 1349–1354.
- Osterwalder, T., Yoon, K. S., White, B. H. and Keshishian, H.** (2001). A conditional tissue-specific transgene expression system using inducible GAL4. *Proceedings of the National Academy of Sciences* **98**, 12596–12601.
- Pandey, U. B. and Nichols, C. D.** (2011). Human Disease Models in *Drosophila Melanogaster* and the Role of the Fly in Therapeutic Drug Discovery. *Pharmacol Rev* **63**, 411–436.
- Paredes, J. C., Welchman, D. P., Poidevin, M. and Lemaitre, B.** (2011). Negative Regulation by Amidase PGRPs Shapes the *Drosophila* Antibacterial Response and Protects the Fly from Innocuous Infection. *Immunity* **35**, 770–779.
- Pende, M., Becker, K., Wanis, M., Saghafi, S., Kaur, R., Hahn, C., Pende, N., Foroughipour, M., Hummel, T. and Dodt, H.-U.** (2018). High-resolution ultramicroscopy of the developing and adult nervous system in optically cleared *Drosophila Melanogaster*. *Nat Commun* **9**, 4731.
- Pesah, Y., Pham, T., Burgess, H., Middlebrooks, B., Verstreken, P., Zhou, Y., Harding, M., Bellen, H. and Mardon, G.** (2004). *Drosophila* parkin mutants have decreased mass and cell size and increased sensitivity to oxygen radical stress. *Development* **131**, 2183–2194.

- Rosell, M., Kaforou, M., Frontini, A., Okolo, A., Chan, Y.-W., Nikolopoulou, E., Millership, S., Fenech, M. E., MacIntyre, D., Turner, J. O., et al. (2014).** Brown and white adipose tissues: intrinsic differences in gene expression and response to cold exposure in mice. *American Journal of Physiology-Endocrinology and Metabolism* **306**, E945–E964.
- Ryoo, H. D., Bergmann, A., Gonen, H., Ciechanover, A. and Steller, H. (2002).** Regulation of *Drosophila* IAP1 degradation and apoptosis by reaper and ubcD1. *Nature Cell Biology* **4**, 432–438.
- Saely, C. H., Geiger, K. and Drexel, H. (2012).** Brown versus White Adipose Tissue: A Mini-Review. *Gerontology* **58**, 15–23.
- Santos, A. J. M., Lo, Y.-H., Mah, A. T. and Kuo, C. J. (2018).** The Intestinal Stem Cell Niche: Homeostasis and Adaptations. *Trends in Cell Biology* **28**, 1062–1078.
- Stobdan, T., Sahoo, D., Azad, P., Hartley, I., Heinrichsen, E., Zhou, D. and Haddad, G. G. (2019).** High fat diet induces sex-specific differential gene expression in *Drosophila Melanogaster*. *PLOS One* **14**, e0213474.
- Susic-Jung, L., Hornbruch-Freitag, C., Kuckwa, J., Rexer, K.-H., Lammel, U. and Renkawitz-Pohl, R. (2012).** Multinucleated smooth muscles and mononucleated as well as multinucleated striated muscles develop during establishment of the male reproductive organs of *Drosophila Melanogaster*. *Developmental Biology* **370**, 86–97.
- Takeuchi, T., Suzuki, M., Fujikake, N., Popiel, H. A., Kikuchi, H., Futaki, S., Wada, K. and Nagai, Y. (2015).** Intercellular chaperone transmission via exosomes

contributes to maintenance of protein homeostasis at the organismal level. *Proc Natl Acad Sci U S A* **112**, E2497–E2506.

**Umar, S.** (2010). Intestinal Stem Cells. *Curr Gastroenterol Rep* **12**, 340–348.

**Wang, W., Liu, W., Wang, Y., Zhou, L., Tang, X. and Luo, H.** (2011). Notch signaling regulates neuroepithelial stem cell maintenance and neuroblast formation in *Drosophila* optic lobe development. *Developmental Biology* **350**, 414–428.

**Wilson, C., Pearson, R. K., Bellen, H. J., O’Kane, C. J., Grossniklaus, U. and Gehring, W. J.** (1989). P-element-mediated enhancer detection: an efficient method for isolating and characterizing developmentally regulated genes in *Drosophila*. *Genes Dev.* **3**, 1301–1313.

**Zaidman-Rémy, A., Hervé, M., Poidevin, M., Pili-Floury, S., Kim, M.-S., Blanot, D., Oh, B.-H., Ueda, R., Mengin-Lecreulx, D. and Lemaitre, B.** (2006). The *Drosophila* Amidase PGRP-LB Modulates the Immune Response to Bacterial Infection. *Immunity* **24**, 463–473.

**Zinke, I., Kirchner, C., Chao, L., Tetzlaff, M. and Pankratz, M.** (1999). Suppression of food intake and growth by amino acids in *Drosophila* : the role of pumpless , a fat body expressed gene with homology to vertebrate glycine cleavage system. *Development* **126**, 5275–5284.